



UPPSALA  
UNIVERSITET

UPTEC W 21047

Examensarbete 15 hp  
September 2021

# Modelling control strategies for chemical phosphorus removal at Tivoli wastewater treatment plant

---

Sara Rosendahl

# Abstract

## Modelling control strategies for chemical phosphorus removal at Tivoli wastewater treatment plant.

-Sara Rosendahl

Wastewater compose an environmental risk as it contains high levels of nutrients, including phosphorus. Wastewater treatment plants (WWTPs) reduce phosphorus by using coagulants that precipitate soluble phosphate into metal phosphate, which is separated by settling. Coagulant flow is regulated by a control strategy, typically feedforward or feedback control. Feedforward is based on incoming wastewater disturbances whereas feedback control uses outgoing process values. Incoming phosphate is hard to measure and can be estimated using soft sensors. Modelling control strategies can help decide which strategy that is most suitable. Models describing phosphorus removal are Activated Sludge Model, ASM2d, and primary clarifier model. ASM2d models phosphorus precipitation and the primary clarifier model settling of particles.

Tivoli WWTP faces challenges to reach effluent requirements of phosphorus. The wastewater flows through an equalisation tank, Regnbågen, before being pumped to Tivoli. Particulate matter settles in Regnbågen, which is removed by reducing the water level in Regnbågen. This rapidly increases incoming particulate load to Tivoli. Tivoli's current control strategy is feedforward proportional to suspended solids. It is suspected, that this strategy overdose coagulant during the emptying of Regnbågen.

The purpose of this thesis was to find the optimal control strategy for phosphorus precipitation at Tivoli WWTP, by using a model-based approach. Control strategies modelled are; feedforward, feedback and these two control strategies combined. Additional issues resolved are 1) calibration of a model that predicts the effect of chemical dosage on effluent phosphorus concentration from the primary clarifier, 2) calibration of a soft sensor, 3) determination of which control strategy that is most suitable.

ASM2d and a primary clarifier model were used to create a model describing chemical phosphorus removal. The calibration matches measured phosphate concentration, but underestimate peaks. The primary clarifier model was calibrated by minimising load differences for phosphate and total suspended solids, and was calibrated satisfyingly. A simplified soft sensor was constructed, described by a linear relationship between phosphate and pH. Three disturbances for feedforward control were analysed; measured phosphate, the soft sensors estimation of phosphate and Tivoli's current control strategy. The optimal control strategy was found through a multi-criteria analysis.

The optimal control strategy is the combined control strategy, when feedforward is proportional to incoming measured phosphate. The performance of all analysed feedforward disturbances were significantly improved when combined with feedback control. Furthermore, consequential error are distinct when the soft sensor miss-predict incoming phosphate concentration. If the phosphate concentration cannot be correctly measured/estimated, feedback control alone has the best performance.

**Keyword:** Wastewater treatment plant, phosphorus precipitation, control strategy, feedforward, feedback, ASM2d and primary clarifier model.

*Division of Industrial Electrical Engineering and Automation, Lund University, Ole Römers väg 1, SE:-223 63, Lund, ISSN 1401-5765.*

# Referat

## Modellering av styrstrategier för kemisk fällning av fosfor vid Tivoli avloppsreningsverk.

- Sara Rosendahl

Avloppsvatten utgör en miljörisk då det innehåller höga halter av näringsämnen, inklusive fosfor. Avloppsreningsverk minskar mängden fosfor genom tillsättning av fällningsmedel som reagerar med löst fosfat, varpå metallfosfat bildas. Metallfosfat avkiljs genom sedimentering. Flödet av fällningsmedel regleras av en styrstrategi, ofta framkoppling eller återkoppling. Framkoppling baseras på inkommande parameterar i avloppsvattnet, medan återkoppling använder utgående processvärden. Inkommande fosfat är svårt att mäta och kan uppskattas med *soft sensors*. Modellering av styrstrategier ger information om vilken strategi som fungerar bäst. Modeller som beskriver kemisk fosforrening är Activated Sludge Model, ASM2d, och försedimenteringsmodell. ASM2d modellerar fosfatutfällning och försedimenteringsmodellen sedimentation.

Tivoli avloppsreningsverk har återkommande haft problem att nå utsläppskrav för fosfor. Avloppsvattnet passerar ett utjämningsmagasin, Regnbågen, innan det når Tivoli. I Regnbågen sedimenterar partikulärt material, och därför sänks nivån i Regnbågen dagligen för att pumpa materialet till Tivoli. Under nedpumpningen ökar inkommande belastningen till Tivoli markant. Tivolis nuvarande styrstrategi är framkoppling proportionell mot suspenderat material, och denna styrstrategi misstänks överdosera fällningsmedel vid nedpumpningar.

Syftet med uppsatsen var att genom modellering hitta en optimal styrstrategi för fällning av fosfat vid Tivoli avloppsreningsverk. Styrstrategier undersökta är; framkoppling, återkoppling samt när dessa två styrstrategier kombineras. Ytterligare angelägenheter genomförda var; 1) kalibrering av en modell som förutsäger effekten av fällningsmedel på utgående fosforkoncentration från försedimenteringsbassängen, 2) kalibrering av en soft sensor, 3) avgöra vilken styrstrategi som är mest lämplig.

ASM2d och en försedimenteringsmodell användes, som tillsammans beskriver kemisk fosforrening. Kalibreringen av ASM2d matchar uppmätt fosfatkoncentration, men underskattar dynamiken. Försedimenteringsmodellen kalibrerades genom att minimera skillnader i massbalanser för fosfat och totalt suspenderat material. Kalibreringen var tillfredsställande. En förenklad soft sensor konstruerades, där en linjär korrelation mellan fosfat och pH används. För framkoppling undersöktes tre parametrar; uppmätt fosfat, soft sensorens uppskattning av fosfat samt Tivoli's nuvarande styrstrategi. Genom en multikriterieanalys avgjordes vilken styrstrategi som var optimal.

Den optimala styrstrategin var en kombinerad styrstrategi, då framkopplingsparametern var uppmätt fosfat. Prestandan för alla framkopplingsparametrar förbättrades avsevärt vid kombinerad återkoppling. Följdfel var tydliga när soft sensoren missförutspådde inkommande fosfat. Slutsatsen blev att ifall inkommande fosfatkoncentrationen inte kan mätas / uppskattas korrekt är återkoppling den bästa styrstrategin.

**Nyckelord:** Avloppsreningsverk, fällning av fosfor, styrstrategier, framkoppling, återkoppling, ASM2d och försedimenteringsmodell.

*Avdelningen för Elektroteknik och Automation, Lunds Universitet, Ole Römers väg 1, SE:-223 63, Lund, ISSN 1401-5765.*

## Preface

This thesis concludes five year long studies at the Master's Programme of Environmental and Water Engineering at Uppsala University and the Swedish University of Agricultural Sciences. The thesis holds 30 credits and is performed at MittSverige Vatten & Avfall under the guidance of Olov Eriksson. Subject reviewer was Ramesh Saagi, postdoctor at the division of Industrial Electrical Engineering and Automation, Lunds University.

First I want thank Olov for kind support throughout the thesis, quick feedback and helping me with sampling of data. I also would like to direct my gratitude towards Ramesh for teaching me the model, your engagement and help with the writing process. Additionally, I want to thank Malin Tuveesson for all your help and creating time for all our discussions. I also want to thank Bengt Carlson for exchanging ideas and very valuable input. Lastly, I would like to thank Anna Maria Kullberg for reading my report, as well as lab and operational staff at Tivoli.

I would also like to thank Tomas Gustavsson and Håkan Wiktorsson at Kemira for input on chemical coagulation, and allowance to publish pictures. Additionally, I want to thank the municipal corporations who helped me fulfil the national analysis.

As my studied are at an end in Uppsala, I would like to thank all my friends for an unforgettable time. My final thanks go to my family, for all the support throughout the thesis and my studies.

*Sara Rosendahl*  
Uppsala, 2021

Copyright© Sara Rosendahl, Division of Industrial Electrical Engineering and Automation, Lund University and the department of Information Technology, Uppsala University. UPTec W 21047, ISSN 1401-5765.

Digitally published in DIVA, 2021, at the Department of Earth Sciences, Uppsala University, Uppsala 2021.

## Populärvetenskaplig sammanfattning

Avloppsvatten innehåller mycket organiskt material och näring i form av fosfor och kväve, och kan därför orskaka övergödning i hav och sjöar. Övergödning kan leda till låga syrenivåer vilket är farligt för vattenlevande organismer. De låga syrenivåerna uppkommer då bakterier som lever i vattnet förbrukar syre vid nedbrytning av organiskt material. Avloppsreningsverk uppgift är att minska mängderna organiskt material och näringsämnen, för att undvika övergödning.

Avloppsreningsverk består typiskt av tre olika reningssteg; ett mekaniskt, kemiskt och biologiskt. Den mekaniska reningen tar bort större material från avloppsvattnet, såsom kvistar, trasor och sand. Den kemiska reningen minskar mängden fosfor från avloppsvattnet. Den biologiska reningen bryter bakterier ner organiskt material, på samma sätt som i naturen. För att den biologiska reningen ska lyckas, är det viktigt att bakterierna har bra förutsättningar för att växa och frodas. Då krävs det att avloppsvattnet inte har brist på näring.

Detta projekt fokuserar på den kemiska reningen. Vid den kemiska reningen tillsätts ett fällningsmedel som reagerar med löst fosfat, varpå metallfosfat fälls ut. Metallfosfaten klumpar ihop sig och bildar kemiska flockar. Dessa flockar sedimenterar, och på detta sätt kan fosfor separeras från avloppsvattnet. För att få en bra avskiljning av fosfor är det viktigt att rätt mängd fällningsmedel tillsätts. För lite fällningsmedel gör att fosforhalten ut från reningsverket är för höga, medan för mycket fällningsmedel leder till näringsbrist för bakterierna i den biologiska reningen. Kemikaliedoseringen sker automatiskt och regleras via styrstrategier, som räknar ut ett flöde av fällningskemikalier.

Två vanliga styrstrategier är framkoppling och återkoppling. Framkoppling styrs proportionellt mot en parameter i inkommande avloppsvatten; vanligen fosfat eller suspenderat material. Inkommande fosfat är svårt att mäta direkt på avloppsreningsverk, men kan uppskattas på plats med *soft sensors*. Soft sensors kombinerar information från andra variabler i inkommande avloppsvatten, och kan då uppskatta inkommande fosfatkoncentration. Återkoppling utgår från avloppsvattnets koncentration av fosfat efter den kemiska reningen, och jämför den uppmätta fosfatkoncentrationen med ett önskat börvärde. Börvärdet är den optimala fosfathalten för bakterierna i den biologiska reningen. Felet mellan uppmätt och önskad fosfatkoncentration används för att beräkna kemikaliedoseringen.

Modellering av det kemiska reningssteget ökar förståelsen kring processerna som sker, och kan därmed ge indikationer på vilken styrstrategi som är mest lämplig. En aktiverad slammodell, ASM2d, och en försedimenteringsmodell har använts i detta projekt. I ASM2d beräknas fällningen av fosfat och i försedimenteringsmodlen beräknas sedimenteringen av partiklar i försedimenteringsbassängen.

Tivoli avloppsreningsverk är det största avloppsreningsverket i Sundsvall. Tivoli har återkommande haft svårigheter med att uppnå riktvärden för utgående fosfathalt. Innan avloppsvattnet når Tivoli passerar det ett utjämningsmagasin, Regnbågen. I Regnbågen är flödet lågt, vilket gör att material som finns i avloppsvattnet sedimenterar. Därför sänks vattennivån i Regnbågen dagligen, och vid nedsänkningen pumpas det sedimenterade materialet upp till Tivoli. Vid nedpumpningen ökar inkommande belast-

ning till Regnbågen markant. Tivolis nuvarande styrstrategi är framkoppling proportionell mot inkommande suspenderat material. Denna styrstrategi misstänks överdosera fällningsmedel vid nedpumpningarna.

Syftet med detta projekt var att hitta en optimal styrstrategi för fällning av fosfat på Tivolis avloppsreningverk. Målet var att modellera flödet av fällningsmedel för de tre styrstrategierna framkoppling, återkoppling samt när framkoppling och återkoppling kombineras. Följande angelägenheter behövdes lösas för att uppnå syftet.

- Utveckla en kalibrerad modell som förutsäger effekten på utgående fosforkoncentrationen från försedimenteringsbassängen då fällningsmedel tillsätts.
- Utveckla en soft sensor som kan förutsäga inkommande koncentration av fosfat till Tivoli.
- Avgöra vilken styrstrategi som är mest lämplig med hänsyn till stabiliteten av utgående fosfatkoncentration till den biologiska reningen, användning av fällningsmedel, produktion av slam och komplexiteten av styrstrategin.

Genom att kalibrera ASM2d och försedimenteringsmodellen erhöles en modell som kan beräkna fosfatkoncentrationen från den kemiska reningen, när fällningsmedel tillsätts. En förenklad soft sensor utvecklades, som inte kombinerade information av alla parametrar i inkommande avloppsvatten utan jämförde parametrarna med inkommande fosfathalt individuellt. Den parametern som bäst korrelerade med inkommande fosfatkoncentration var pH. Genom pH kunde variationerna i inkommande fosfat förutses, men förutsägelsen underskattade dynamiken i fosfatkoncentrationen. Som framkopplingsparameter användes den nuvarande styrstrategin, uppmätt fosfat samt soft sensorens uppskattning av fosfat. En multikriterieanalys konstruerades för att avögra vilken av styrstrategierna som var den optimala.

Resultatet blev att den kombinerade styrstrategin var den bästa, då framkoppling styrdes proportionellt mot uppmätt fosfat. Den näst bästa styrstrategin var återkoppling. Tredje bäst var framkoppling styrd proportionellt mot uppmätt fosfat. Framkoppling som inte styrdes proportionellt mot uppmätt fosfat presterade generellt dåligt, och följdfel från soft sensors estimeringen av inkommande fosfat var tydliga. Sämst var den nuvarande styrstrategin där framkopplingen styrs proportionellt mot suspenderat material. Alla tre styrstrategier baserade på framkoppling förbättrades markant när framkopplingen kombinerades med återkoppling.

Det kunde därmed fastställas att styrstrategins prestanda påverkas mycket av framkopplingsparametern - i de fall då inkommande fosfat inte korrekt kan uppskattas är det bättre att endast använda återkoppling som styrstrategi. Rekommenderade styrstrategier till Tivoli är 1) kombinerad styrstrategi där framkopplingen styrs proportionellt mot uppmätt fosfat, och tillsätta en utredning ifall inkommande fosfat kontinuerligt kan mätas eller utveckla en traditionell soft sensor, 2) endast återkoppling, 3) kombinerad styrstrategi där framkoppling styrs proportionellt mot pH, men först förbättra korrelationen mellan pH och inkommande fosfat.

# Contents

- 1 Introduction** **1**
  - 1.1 Purpose and issues . . . . . 1
  - 1.2 Boundaries . . . . . 2
  
- 2 Theory** **2**
  - 2.1 Wastewater . . . . . 2
    - 2.1.1 Phosphorus in wastewater . . . . . 3
  - 2.2 Wastewater treatment process . . . . . 3
    - 2.2.1 Mechanical treatment . . . . . 3
    - 2.2.2 Biological treatment . . . . . 4
    - 2.2.3 Chemical treatment . . . . . 5
  - 2.3 Removal of phosphorus . . . . . 5
    - 2.3.1 Settling of particles . . . . . 6
  - 2.4 Modelling of WWTP . . . . . 7
    - 2.4.1 Model setup . . . . . 7
    - 2.4.2 ASM2d: Activated Sludge Model No. 2d . . . . . 9
    - 2.4.3 Primary clarifier model . . . . . 10
  - 2.5 Control strategies . . . . . 11
    - 2.5.1 Feedback and & feedforward control . . . . . 11
    - 2.5.2 Control strategies for phosphorus precipitation . . . . . 13
  - 2.6 Controller tuning approach - The Lambda method . . . . . 14
  
- 3 Background** **15**
  - 3.1 National analysis: Experiences from other WWTPs . . . . . 15
  - 3.2 Tivoli WWTP . . . . . 17
    - 3.2.1 Purpose and problems with the equalisation tank . . . . . 17
    - 3.2.2 Current control strategy . . . . . 18
    - 3.2.3 Tivoli’s issue with irregular load . . . . . 18
  
- 4 Method** **18**
  - 4.1 Sampling of data . . . . . 19
    - 4.1.1 Data measurements . . . . . 19
    - 4.1.2 Sampling campaign . . . . . 20
  - 4.2 Model calibration . . . . . 21
    - 4.2.1 Influent characterisation . . . . . 21
    - 4.2.2 Addition of coagulant . . . . . 21
      - 4.2.3 ASM2d model . . . . . 22
        - 4.2.3.1 Adjust stoichiometric coefficients for aluminium based precipitation . . . . . 22
        - 4.2.3.2 Determine phosphate concentration to calibrate ASM2d by . . . . . 23
        - 4.2.3.3 Rate constant for precipitation and redissolution . . . . . 23
    - 4.2.4 Primary clarifier model . . . . . 24
      - 4.2.4.1 Adjust stoichiometric coefficients for aluminium based precipitation . . . . . 24
      - 4.2.4.2 Mass balances . . . . . 25

4.3	Prediction of phosphate . . . . .	27
4.4	Control strategies . . . . .	29
4.4.1	Feed forward . . . . .	29
4.4.2	Feedback . . . . .	31
4.4.2.1	Tuning the PI- controller . . . . .	31
4.4.3	Feedback combined with feedforward . . . . .	33
4.5	Multi-criteria analysis . . . . .	34
<b>5</b>	<b>Results and discussion</b>	<b>35</b>
5.1	Model calibration . . . . .	35
5.1.1	ASM2d . . . . .	35
5.1.2	Primary clarifier model . . . . .	36
5.2	Prediction of phosphate . . . . .	37
5.3	Combined feedforward with feedback control . . . . .	40
5.4	Evaluation of the control strategies and multi-criteria analysis . . . . .	41
5.5	Consequential errors . . . . .	44
5.5.1	Estimation of phosphate . . . . .	44
5.5.2	Comparison over model parameters for ASM2d . . . . .	45
5.6	Improvements and uncertainties . . . . .	46
<b>6</b>	<b>Conclusions</b>	<b>47</b>
	<b>References</b>	<b>49</b>
	<b>Appendix A Background: National analysis</b>	<b>1</b>
	<b>Appendix B Method: Data</b>	<b>1</b>
	<b>Appendix C Method: Soft sensor - prediction of phosphate</b>	<b>1</b>
	<b>Appendix D Result: Estimations of phosphate</b>	<b>1</b>
	<b>Appendix E Result: Performance of the control strategies</b>	<b>1</b>

# 1 Introduction

The importance of well treated wastewater increases as the anthropogenic impact on the world grows (UNESCO , 2020). Wastewater contains high levels of nutrients and pathogens, and therefore compose a risk for human health and environment. Phosphorus is often the limiting nutrient in surface waters, and increasing levels of phosphorus will therefore contribute to eutrophic conditions (Welch , 1980). To avoid eutrophication it is essential that wastewater treatment plants (WWTP) are successful in removing phosphorus from the wastewater. One of the more efficient processes to remove phosphorus is through coagulation, in which soluble phosphate is precipitated into particulate material that can be removed by settling (Manamperuma et al , 2017).

Modelling control strategies for chemical phosphorus removal can improve the performance of phosphorus precipitation, and help decide which control strategy that is most suitable. A control strategy regulates the flow of coagulant used to precipitate phosphorus. Feedforward control is commonly used for chemical phosphorus removal, and is based on the characteristics of incoming wastewater (SvensktVatten , 2010c). Incoming soluble phosphate is hard to measure online at WWTPs, but can be estimated using soft sensors (IVL , 2008). Studies have shown that feedback control can improve chemical phosphorus removal, as feedback control tends to reduce and stabilise effluent phosphate concentration from the primary clarifier as well as reduce coagulant consumption (Ingildsen , 2002) & (Liu & Ratnaweera , 2016). Models describing chemical phosphorus removal are Activated Sludge Model, ASM2d, and a primary clarifier model. ASM2d calculates the precipitation of phosphorus and the primary clarifier model calculates the settling of particles (Henze, et. al. , 2002) & (Otterpohl et al , 1994).

Tivoli WWTP faces challenges to reach effluent requirements for phosphorus concentration. These challenges are believed to partly derive from the coagulation process, where feedforward control is currently used to regulate the dosing of precipitation chemicals before the primary clarifier. The coagulation process at Tivoli is affected by an equalisation tank, Regnbågen, which creates peaks of incoming particulate solid loads. It is suspected that the current control strategy overdose coagulant during these peaks and thus excess phosphorus removal, which affects the following biological processes. Tivoli WWTP therefore has a need to optimise the control strategy for chemical phosphorus removal.

## 1.1 Purpose and issues

The purpose of this thesis is to find the optimal control strategy for chemical precipitation of phosphorus at Tivoli WWTP using a model-based approach. The goal is to model three control strategies that regulate the dosage of precipitation chemicals to the primary clarifier. The control strategies investigated are 1. Feedforward control based on incoming wastewater characteristics; 2. Feedback control based on effluent phosphate concentration from the primary clarifier; and 3. A combination of feedforward and feedback control strategies.

Issues to be resolved in order to fulfil the purpose of the thesis are;

1. Develop a calibrated model that predict the effect of chemical dosage on phos-

phorus concentration from the primary clarifier.

2. Develop a soft sensor that predict incoming soluble phosphate concentration to Tivoli WWTP.
3. Determine which control strategy that is most suitable with regard to the stability of the effluent phosphate concentration from the primary clarifier, coagulant dosage, sludge production and the complexity of the control strategy.

In addition to this, a national analysis of commonly used control strategies at WWTPs in Sweden will be made.

## 1.2 Boundaries

The project will focus on chemical phosphorus removal using chemical precipitation. Therefore, only a basic description of the general wastewater treatment process will be covered regarding mechanical and biological treatment. Important processes for a WWTP's general performance that do not directly influence chemical precipitation, such as sludge treatment and production, will be skipped completely.

Furthermore, the theory will be focused on the treatment steps that Tivoli uses. Tivoli uses a simple activated sludge treatment step in the biological treatment, with no expanded nitrogen removal process. Only theory regarding activated sludge is therefore covered. Similarly, Tivoli uses pre-precipitation and thus little attention will be given to simultaneous and post-precipitation.

ASM2d and a primary clarifier model are used in this thesis. Only precipitation processes in ASM2d are explained in this thesis. Other biological processes are not elaborated as ASM2d model is used only to simulate chemical precipitation and redissolution of phosphate happening in the primary clarifier.

## 2 Theory

This chapter covers general information about wastewater and the treatment of wastewater. The chapter also presents information about the used models, ASM2d and the primary clarifier. Furthermore are control strategies, their implementation in WWTPs as well as current research covered. Lastly, is the Lambda method described, which is a controller tuning approach.

### 2.1 Wastewater

Wastewater consists mainly of water that is used in households but might also contain stormwater that is either lead into the sewer network or leaks into the pipes (SvensktVatten , 2010a). The characteristics of wastewater depends largely on the characteristics of the community and industries connected to the sewer network, and the condition of the sewage system (SvensktVatten , 2010a). Generally, wastewater contains high concentrations of nutrients and organic matter, as well as heavy metals, organic toxicants and pathogens. The nutrients, phosphorus and nitrogen, increase the risk of eutrophication in recipients which can cause low dissolved oxygen levels. The organic matter

requires much oxygen during degradation, further reducing oxygen levels in recipients. Low oxygen levels are problematic for higher developed organisms. Dead zones are areas where the oxygen level is reduced so no or little aquatic life can live (Welch , 1980).

### 2.1.1 Phosphorus in wastewater

Phosphorus is present in wastewater in both dissolved and particulate states. Particles smaller than 1.2  $\mu\text{m}$  are considered dissolved (Metcalf & Eddy , 2014). Dissolved phosphorus can be both organic and inorganic. Dissolved inorganic phosphorus is known as orthophosphate,  $\text{PO}_4\text{-P}$ , which is chemically reactive soluble phosphate. Orthophosphates are salts of orthophosphoric acid,  $\text{H}_3\text{PO}_4$ .

Polyphosphates and organic phosphorus are also present in wastewater. Polyphosphates are polymers of  $\text{H}_3\text{PO}_4$  and breaks down to orthophosphates. The organic phosphorus can also be transformed to orthophosphates during the biological treatment (SvensktVatten , 2010b).

Organic phosphorus is usually bound to colloidal and suspended particles (Kemira , 2020). Colloidal particles are around 0.01 - 1  $\mu\text{m}$  and are thus smaller than suspended particles. The difference between particle types is whether gravity affects the particle enough to settle. Colloidal particles are kept in suspension by Brownian motion<sup>1</sup> and will therefore not settle. The colloidal particles are also negativity charged, thus repelling each other. Even though colloidal particles are small enough to pass as dissolved, they are usually considered to be particulate. The distinction between colloidal particles and dissolved material is not standardised (Metcalf & Eddy , 2014).

## 2.2 Wastewater treatment process

The treatment process of wastewater varies largely between WWTPs, but typically consists of three steps; mechanical, biological and chemical (SvensktVatten , 2010a).

### 2.2.1 Mechanical treatment

The primary treatment is mechanical and the purpose is to remove large material that can cause damage to the treatment process (SvensktVatten , 2010b). A typical mechanical treatment process consists of three steps; wastewater passing through screens, a sand trap or grit chamber that is followed by a primary clarifier. A primary clarifier is a basin in which heavier material is allowed to settle. These steps are shown in figure 1. The screens remove large materials such as rags and twigs. Sand traps are usually aerated and designed to make heavier particles settle, such as sand and coffee grounds. Mechanical treatment removes around 30-70 % of suspended solids and 30 % of BOD (biochemical oxygen demand), (Kemira , 2020).

---

<sup>1</sup>Brownian motion is a random movement of small particles in a fluid. Colloidal particles are bombarded by water molecules driven by thermal motion. This keeps the particles in suspension (Metcalf & Eddy , 2014).

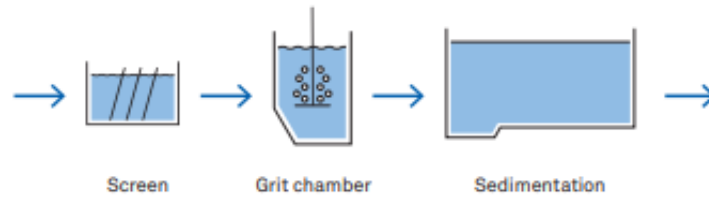


Figure 1: Illustration of the primary, mechanical treatment (Kemira , 2020).

### 2.2.2 Biological treatment

Biological treatment is typically the secondary treatment, and the purpose is to remove organic matter (Kemira , 2020). Organic matter is oxidised by microorganisms that consume substrate for cell growth and metabolism. In addition to substrate, microorganisms also need nutrients for cell growth and metabolism. Most of the microorganisms are heterotrophic and undergo respiration. As microorganisms consume substrate, organic material is transformed into carbon dioxide. Most of the microorganisms are bacteria, but higher developed organisms such as protozoa and metazoa can also be present. The composition of bacteria in wastewater is ever changing due to variations in incoming wastewater composition and process conditions inside the WWTP. More diverse bacteria communities and presence of higher developed organisms are associated with better performance of the biological treatment (SvensktVatten , 2010b). The biological treatment performance is typically improved when there is a steady incoming load of organic matter and nutrients to the treatment step (Kemira , 2020).

Figure 2 shows the layout of the biological treatment. During aeration the growth rate of bacteria is increased, which reduces organic matter present in the wastewater. The sedimentation occurs at the secondary clarifier, in which flocs consisting of bacteria are formed and settles. Some of the bacteria are returned to aeration through the return sludge, and the rest is surplus sludge which is treated separately. The process of using the return sludge is called activated sludge and makes the bacteria composition more diverse. By increasing the time bacteria spend in the biological treatment, it enables higher developed organisms to evolve (SvensktVatten , 2010b).

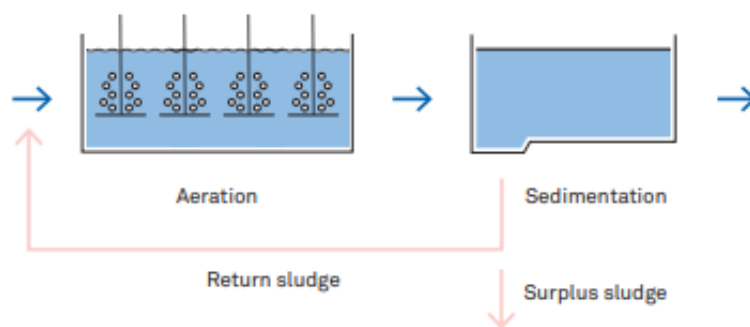


Figure 2: Illustration of the biological treatment process (Kemira , 2020).

The benchmark ratio for optimal growth of bacteria between BOD<sub>7</sub>, nitrogen and phosphorus is 100:5:1 during aeration. A lack of any of these variables will therefore deteriorate the bacteria's ability to grow (SvensktVatten , 2010b).

During the biological treatment up to 90 % of the organic matter can be removed. Since bacteria consume nutrients, a reduction of 25-40 % for phosphorus and nitrogen also takes place during the biological treatment (SvensktVatten , 2010a).

### 2.2.3 Chemical treatment

The main purpose of chemical treatment in municipal WWTPs is to remove phosphorus, but the chemical treatment also reduces organic matter and bacteria. The treatment process is known as tertiary treatment, but can be placed both before (pre-precipitation), during (simultaneous precipitation) and after (post-precipitation) the biological treatment step (SvensktVatten , 2010b). The pre-precipitation process is shown in figure 3. The coagulant is a chemical precipitant and, when mixed with wastewater, allows soluble phosphate to form chemical floc and precipitate. The mixing can occur in the clarifier itself or in a separate flocculation chamber. The flocs are separated by settling in a clarifier. The treatment efficiency for phosphorus removal is >90 % for pre-precipitation (Kemira , 2020).

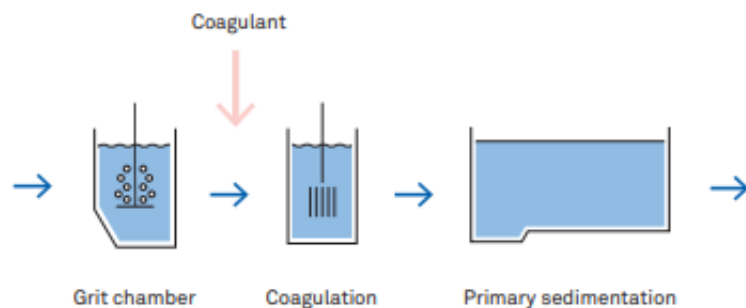


Figure 3: An illustration of the chemical treatment process (Kemira , 2020).

Pre-precipitation allows the biological step to be smaller, as much of the organic matter is precipitated and separated before the biological treatment. This leads to reduced energy costs, due to less aeration in the biological step (SvensktVatten , 2010b). Some WWTPs experience more control over the biological treatment step with pre-precipitation, since it is possible to adjust incoming phosphorus concentration to the biological treatment by adding chemical dosage (Kemira , 2020). Pre-precipitation also results in higher biogas production, because more organic matter is present in the chemical sludge and therefore not transformed into carbon dioxide. There are two main disadvantages with pre-precipitation. The first is risk of overdosing the coagulant, which will result in a lack of phosphorus in the biological treatment and limit bacterial growth. The second is the increased production of chemical sludge, which if not used for biogas production will increase costs (SvensktVatten , 2010b).

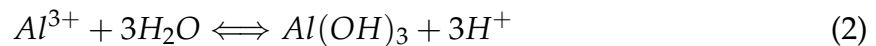
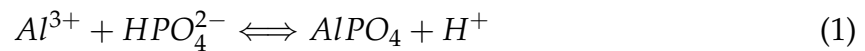
## 2.3 Removal of phosphorus

There are three main reactions that occurs when a coagulant is added to wastewater; particle, -phosphorus, and hydroxide precipitation (SvensktVatten , 2010b). Particle precipitation occurs when the surface charge of colloids are destabilised by a cation from the coagulant, in a process called charge neutralisation. This process is very fast

and takes about 0.01 - 1 seconds. The neutralised particles allows particles to aggregate. The aggregate adsorbs more particles and forms chemical floc, which is removed by settling (Kemira , 2020).

Phosphorus precipitation removes orthophosphate, as shown in equation 1 for an aluminium based coagulant. Orthophosphate reacts with cations and form aluminium phosphate, a salt that is hard to dissolve. The precipitate is however dependent on pH, and it's lowest solubility is around a pH of 6 (SvensktVatten , 2010c). The formation of aluminium phosphate takes less than 1 second, and the precipitate is removed by settling. From equation 1 it is clear that the theoretical molar ratio between aluminium and phosphate is 1:1. In practice, a ratio of 1-1.5 moles per aluminium is typically required, as aluminium also reacts with other compounds within the wastewater (Kemira , 2020).

The formation of metal hydroxide precipitation occurs when metal salts react with water, equation 2. Aluminium hydroxide floc will form, and as it settles it sweeps through the wastewater and colloidal particles are adsorbed onto the floc. This process is called sweep coagulation. The reaction time is around 1-7 seconds (Kemira , 2020) (Metcalf & Eddy , 2014). The reaction releases hydrogen ions, which lowers alkalinity and pH. This can affect the metal hydroxide precipitation, since its solubility is sensitive to pH. The precipitation ranges between a pH of 5 to 7, with the lowest solubility around a pH of 6. Some WWTPs overdose coagulant to achieve a pH with low solubility (Metcalf & Eddy , 2014). However, coagulants contain heavy metals and are costly. Therefore, many WWTPs avoid overdosing coagulant.



There are immensely more water molecules than orthophosphate present in wastewater. Therefore, most of the coagulant react with water (equation 2), instead of orthophosphate. To ensure a good reduction of dissolved phosphorus, it is important to have a swift mixing when the coagulant is added. Flocs are brittle and break easily. After flocculation it is therefore important to have a slow and steady flow (Kemira , 2020).

### 2.3.1 Settling of particles

The four main types of settling are discrete particle settling, flocculant settling, hindered settling and compression. Discrete particle settling removes larger particles, such as sand. Particles in discrete particle settling does not interfere with other particles. Flocculant settling is applied when coagulants are used, and removes chemical floc. During this settling particles flocculate which enables a faster settling. Hindered settling occurs after the biological treatment, where the concentration of particles is big enough to create interparticle forces that hinder settling on neighbouring particles. Compression happens in lower layers of the surplus sludge (Metcalf & Eddy , 2014).

For a particle to settle, its critical settling velocity must be equal to or greater than the surface load according to equation 3. The settling velocity can be estimated with Stokes equation, equation 4. It should be noted that the settling velocity of a particle is quadratic proportional to its diameter. Flocculation is therefore crucial for a good

settling. Stoke's equation assumes that particles are round, which usually is not true. Therefore Stoke's equation is rarely fit to be used in practical applications, but it gives a good overlook over which parameters that effect settling velocity (Metcalf & Eddy , 2014) (SvensktVatten , 2010b).

$$v_{critical} = \frac{h_o}{\tau} = \frac{h_o Q}{h_o A} = \frac{Q}{A} = Surface\ Load \quad (3)$$

$$v_{settling} = \frac{g(\rho_p - \rho_f)d^2}{18\mu} \quad (4)$$

In the equations are  $v_{critical}$  = settling velocity of particle [m/h],  $h_o$  = height of clarifier basin [m],  $\tau$ = detention time [h],  $Q$  = flow [ $m^3/h$ ],  $A$  = area of clarifier basin [ $m^2$ ],  $v_{settling}$  = settling velocity [m/s],  $g$  = acceleration due to gravity [ $m/s^2$ ],  $\rho_p$  = density of particle [ $kg/m^3$ ],  $\rho_f$  = density of fluid [ $kg/m^3$ ],  $d$  = diameter of particle [m] and  $\mu$ = the viscosity of fluid [ $kg/(s \cdot m)$ ].

## 2.4 Modelling of WWTP

The importance of optimising the wastewater treatment process continues to grow, as the requirements on treatment efficiency becomes stricter and incoming load to WWTPs increase. The technologies becomes more advanced, which leads to a need to have more control over the processes. Modelling wastewater treatment plants can significantly increase the understanding behind the processes that occur, improve the performance of the WWTP as well as reduce costs (Vanrolleghem , 1999).

### 2.4.1 Model setup

Models used in this project are ASM2d and a primary clarifier model, both typically implemented in Benchmark Simulation Model No. 2, BSM2, which is a simulation environment in Matlab-Simulink. BSM2 is developed for benchmarking control strategies at WWTPs and designed to view the WWTP as one unit where each treatment process affect and interact with other processes. BSM2 typically includes all processes happening at a WWTP, including the biological treatment step and sludge treatment (Nopens et al , 2010).

The model layout used in this thesis is seen in figure 4. Input data can be chosen to be either constant or dynamic. The module *Addition of coagulant* adds coagulant flow and concentration of metal hydroxide within the coagulant to the model. The module *ASM2d* contains the ASM2d model, and calculates the precipitation of phosphate, and how much metal phosphate that is formed. The module *primary clarifier model* calculates the settling of particles, including chemical floc, in the primary clarifier.

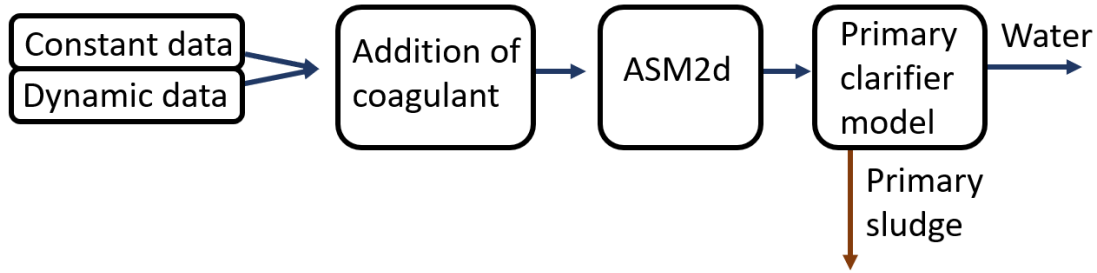


Figure 4: Model layout.

The model setup includes a Simulink-model, run-file, C-files, initialisation files and influent data. The model set up is described in table 1.

Influent data consists of state variables, table 2. The state variables are divided into dissolved components and particulate components, and mainly consists of phosphorus, nitrogen and carbonaceous material, described by COD (chemical oxygen demand), (Henze, et. al. , 2002).

Table 1: Files included in the model setup.

File- type	Description
Run-file	
<i>run_primaryclarifier.m</i>	Runs the simulation in Matlab-Simulink.
Simulation model	
<i>primaryclarifier.slx</i>	Model layout in Simulink.
C-files	
<i>asm2d_bsm2.c:</i>	Contains the ASM2d model.
<i>primclar_bsm2.c:</i>	Contains the primary clarifer model.
Initalisation files	
<i>asm2dinit_bsm2:</i>	Defines model parameters for the ASM2d model.
<i>primclarinit_bsm2:</i>	Defines model parameters for the primary clarifier model.
Influent data	
<i>constinfluent_bsm2:</i>	A constant mean value of influent data.
<i>dynamicludent_bsm2:</i>	Dynamic influent data.

Table 2: State variables.

<b>Dissolved components:</b>		
$S_{O_2}$	Dissolved oxygen	$\text{g O}_2 \text{ m}^{-3}$
$S_F$	Readily biodegradable substrate	$\text{g COD m}^{-3}$
$S_A$	Fermentation products (acetate)	$\text{g COD m}^{-3}$
$S_{NH_4}$	Ammonium	$\text{g N m}^{-3}$
$S_{NO_3}$	Nitrate (plus nitrite)	$\text{g N m}^{-3}$
$S_{PO_4}$	Phosphate	$\text{g P m}^{-3}$
$S_I$	Inert, non-biodegradable organics	$\text{g COD m}^{-3}$
$S_{ALK}$	Bicarbonate alkalinity	$\text{mole HCO}_3^- \text{ m}^{-3}$
<b>Particulate components:</b>		
$X_I$	Inert, non-biodegradable organics	$\text{g COD m}^{-3}$
$X_S$	Slowly biodegradable substrate	$\text{g COD m}^{-3}$
$X_H$	Heterotrophic biomass	$\text{g COD m}^{-3}$
$X_{PAO}$	Phosphorus-accumulating organisms, PAO	$\text{g COD m}^{-3}$
$X_{PP}$	Stored poly-phosphate pf PAO	$\text{g P m}^{-3}$
$X_{PHA}$	Organic storage products of PAO	$\text{g COD m}^{-3}$
$X_{AUT}$	Autotrophic, nitrifying biomass	$\text{g COD m}^{-3}$
$X_{MeOH}$	Metal hydroxide, $\text{Me(OH)}_3$	$\text{g Me(OH)}_3 \text{ m}^{-3}$
$X_{MeP}$	Metal phosphate', $\text{MePO}_4$	$\text{g MePO}_4 \text{ m}^{-3}$
$X_{TSS}$	Particulate material as model component	$\text{g TSS m}^{-3}$

### 2.4.2 ASM2d: Activated Sludge Model No. 2d

ASM2d is developed by Henze et al (2000). The model portrays simultaneous precipitation and redissolution of phosphate together with several biological processes. ASM2d is an expansion of ASM1 (Activated Sludge Model No. 1), that describes carbon oxidation, nitrification and denitrification within an activated sludge system. ASM1 models the growth of biomass, decay, ammonification of organic nitrogen and hydrolysis. The growth rates of microorganisms in ASM1 and expansions are mainly based on the Monod equation, equation 5, where  $\mu$  = growth rate of bacteria [ $\text{g } X_S (\text{g } X_H)^{-1} \text{ d}^{-1}$ ],  $\mu_{max}$  = maximal growth rate [ $\text{g } X_S (\text{g } X_H)^{-1} \text{ d}^{-1}$ ],  $K_S$  = half velocity constant [ $\text{g COD } S_s \text{ m}^{-3}$ ] and  $S$  = available substrate [ $\text{g COD m}^{-3}$ ].

$$\mu = \mu_{max} \frac{S}{K_S + S} \quad (5)$$

The expansion to ASM2d includes biological phosphorus removal, denitrifying phosphorus accumulating organisms as well as chemical precipitation and redissolution of phosphorus. Biological activity is neglected in this thesis. Therefore, only theory concerning the process rate of chemical precipitation and redissolution will be described below. For a description covering biological activity it is referred to (Henze, et. al. , 2002).

Precipitation and redissolution of phosphate,  $S_{PO_4}$ , are processes that can be reversed. At steady state they are in equilibrium, see equation 6.



The process rates of precipitation and redissolution,  $\rho_{PRE}$  &  $\rho_{RED}$ , are modelled with equation 7 & 8 respectively.  $K_{PRE}$  and  $K_{RED}$  are rate constants for precipitation and redissolution.  $K_{ALK}$  is a saturation coefficient for alkalinity.  $K_{PRE}$  is measured in  $[m^3 g(Me(OH_3)^{-1} d^{-1})]$ ,  $K_{RED}$  in  $[d^{-1}]$  and  $K_{ALK}$   $[mole HCO_3^{-1} m^{-3}]$ .

$$\rho_{PRE} = k_{PRE} \cdot S_{PO_4} \cdot X_{MeOH} \quad (7)$$

$$\rho_{RED} = k_{RED} \cdot X_{MeP} \cdot \frac{S_{ALK}}{K_{ALK} + S_{ALK}} \quad (8)$$

### 2.4.3 Primary clarifier model

The primary clarifier model is based on Otterpohl & Freund (1992) and Otterpohl et al (1994). It assumes a completely mixed tank in which no biological activity occurs. It also assumes that concentrations of incoming soluble components remain unchanged, and that incoming flow rate is equal to the combined flow rate of effluent wastewater and primary sludge, figure 5.

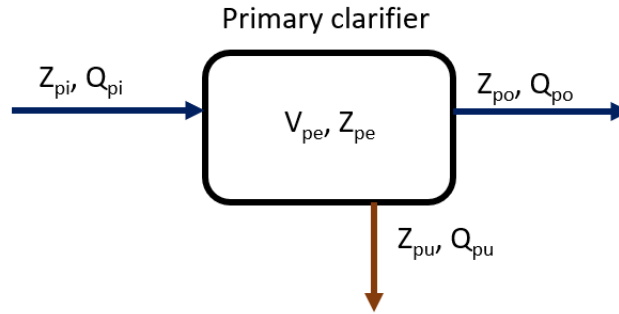


Figure 5: Primary clarifier model layout.

Primary effluent concentration,  $Z_{po,k}$ , is the overflow from the tank and is calculated according to equation 9, whereas effluent primary sludge concentration,  $Z_{pu,k}$ , is the underflow according to equation 10 (Otterpohl et al , 1994).

$$Z_{po,k}(t) = f_k Z_{pi,k}(t) \quad (9)$$

$$Z_{pu,k}(t) = \left( (1 - f_k) \frac{Q_{pi}(t)}{Q_{pu}(t)} + f_i \right) Z_{pc,k}(t) \quad (10)$$

$f_k$  is the effluent concentration factor and is given by equation 11 where  $f_{sx,k}$  is 0 for all soluble fractions and 1 for all particulate fractions except  $X_S$  where it is 0.5.  $\eta_{CODp}$  is the particulate COD removal efficiency, and is given by the fraction of COD removal efficiency,  $\eta_{COD}$ , and  $f_x$ , which is a mean fraction of particulate COD,  $COD_{part}$ , and total COD,  $COD_{tot}$ , equation 12 - 14.

$$f_k = 1 - \frac{\eta_{CODp}}{100} f_{sx,k} \quad (11)$$

$$\eta_{CODp} = \frac{\eta_{COD}}{f_x} \quad (12)$$

$$\eta_{COD}(t) = f_{corr}(2.88 \cdot f_x - 0.118) \cdot (1.45 + 6.15 \cdot \ln(t_h) \cdot 24 \cdot 60) \quad (13)$$

$$f_x = \frac{COD_{part}}{COD_{tot}} \quad (14)$$

The particulate COD removal efficiency is described by the correction factor removal efficiency,  $f_{corr}$ , which has a value of 0.65.  $t_h$  is a mean hydraulic retention time and is calculated as in equation 15, where  $V_{pe}$  is the volume of the reactor and  $Q_m$  the mean flow, which is calculated according to equation 16.  $Q_i$  is the total outflow from the primary clarifier and  $t_m$  is a time constant = 3/24.

$$t_h(t) = \frac{V_{pe}}{Q_m(t) + 0.001} \quad (15)$$

$$\frac{dQ_m(t)}{dt} = \left( Q_{pi}(t) - Q_m(t) \right) \frac{1}{t_m} \quad (16)$$

$Q_{pu}$  is the flow rate of the primary sludge. It is proportional to the influent flow rate,  $f_{PS}$ , and is estimated to 0.007, according to equation 17.

$$Q_{pu} = f_{PS} = 0.007 \quad (17)$$

## 2.5 Control strategies

The choice of control strategy has a big impact on the performance of chemical phosphorus removal (SvensktVatten , 2010c). An optimised control strategy can increase the stability of effluent phosphorus concentration from the primary clarifier and reduce the risk of overdosing coagulant. Overdosing coagulant are associated with lack of phosphorus in biological treatment, higher costs, increased sludge production and higher presence of heavy metals in the primary sludge (SvensktVatten , 2010c).

### 2.5.1 Feedback and & feedforward control

Common control strategies in industrial processes are feedback control and feedforward control. Feedback control regulators use the error (difference between the output value from the process and the desired setpoint) to calculate the control signal. A feedforward controller calculates the control signal using incoming characteristics.

Figure 6 illustrate a block schedule for a feedback regulator.  $S$  represents the system, and  $y$  is the systems outgoing process value.  $R$  is the reference value and  $e$  is the error between the  $r$  and  $y$ .  $K_{FB}$  is the proportional gain from the regulator and  $u$  is the calculated control signal. A proportional feedback regulator, called P-regulator, calculates the control signal according to equation 18 and 19, where  $u_0$  is the offset-signal.

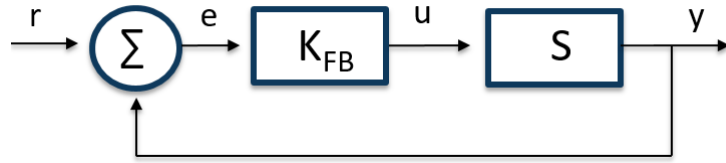


Figure 6: Block schedule over a feedback regulator.

$$u = K_{FB} \cdot e + u_0 \quad (18)$$

$$e = r - y \quad (19)$$

The gain decides how much the proportional feedback will affect the control signal. The P-regulator can compensate disturbances in the process, but cannot eliminate them. A PI-regulator, described in equation 20, introduces an integrating term that is proportional to the error value and eliminates disturbances, but can create instability (Torkel & Ljung , 2006) & (SvensktVatten , 2010c).

$$u = K(e + u_0 + \frac{1}{T_I} \int e(t)dt) \quad (20)$$

$T_I$  is integral time and decides how much the integrating term will influence the control signal.

Figure 7 illustrates a block schedule for a feedforward regulator. Feedforward control uses incoming characteristics, which in this context can be seen as a disturbance, to regulate a control signal. Feedforward control steers the regulator proportional to the disturbance according to equation 21, where  $K_{FF}$  is the gain and  $d$  is the disturbance the regulator is proportional to. Therefore, using feedforward control disturbances can be compensated immediately. However, feedforward control has no control over the outgoing process value in contrast to feedback control (Torkel & Ljung , 2006).

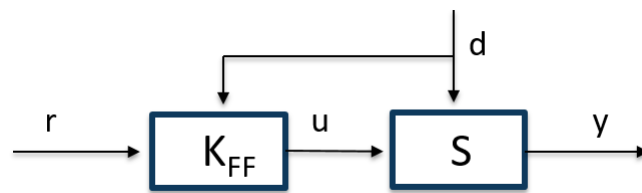


Figure 7: Block schedule over a feedforward regulator.

$$u = K_{FF} \cdot d \quad (21)$$

Feedback control can be combined with feedforward control. Figure 8 illustrates a block schedule for a regulator using combined feedback and feedforward control.

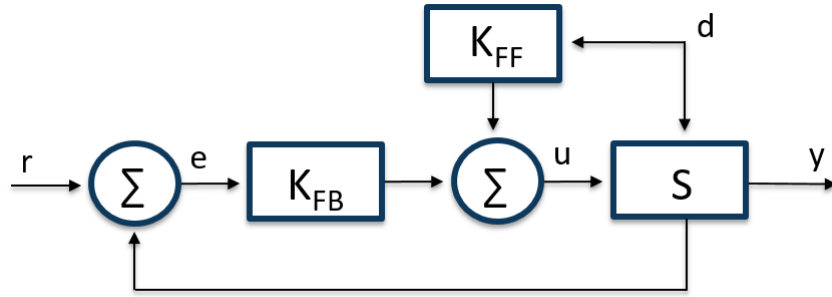


Figure 8: Block schedule over a combined feedforward and feedback regulator.

### 2.5.2 Control strategies for phosphorus precipitation

Control strategies generally used for phosphorus precipitation are time-based, feedforward and feedback control. The strategies can be combined with each other.

In time-based control the dosage of coagulant is a function of time, equation 22 & 23. The control signal,  $u$ , is the flow rate of coagulants, which is the estimated amount of coagulant the regulator calculated should be dosed. Incoming load is higher during daytime, and time-based control is a simple strategy to compensate for the extra load (SvensktVatten , 2010c).

$$u = K(t) \quad (22)$$

$$K(t) = k1(\text{daytime}) \quad (23)$$

$$k2(\text{nighttime})$$

Feedforward is commonly used for phosphorus precipitation. Incoming wastewater characteristics, such as flow or incoming pollutant load, are used to calculate control signal. Equation 24 shows the control signal when it is proportional to incoming phosphate load (SvensktVatten , 2010c).

$$u = K_{FF} \cdot Q_{in} \cdot PO_{4,in}P \quad (24)$$

Feedback control regulators uses effluent phosphate concentration from the primary clarifier or flocculation chamber to calculate an optimal control signal (SvensktVatten , 2010c). Even though WWTPs measure effluent phosphate concentration from the WWTP, these are rarely used for real-time control purposes. This might be due to time lag between dosing and effluent phosphate concentration from the WWTP (Ratnaweera & Fettig , 2005).

Ingildsen (2002) compared four control strategies for chemical phosphorus removal. The first strategy was a constant dose of coagulants, and the second and third was feedforward control proportional to incoming 1) flow 2) phosphate load. The fourth control strategy used a PI regulator measuring phosphate as process value. The phosphate sensor was placed at the end of the flocculation chamber to reduce time lag. The study was carried out at Källby WWTP, which uses post-precipitation. The result

showed that feedback control had the best performance, and could almost perfectly match the desired setpoint. It also consumed less coagulant. Feedforward control based on incoming phosphate load performed second best, followed by feedforward proportional to flow.

Liu & Ratnaweera (2016) compared feedforward control with a combined strategy of feedforward and feedback control, for a WWTP and a drinking water treatment plant, DWTP. The dosage was modelled empirically as a function of flow, incoming suspended solids, pH, conductivity, phosphate, temperature, interaction among variables and variables squares. When the combined control strategy was studied, the process values from the feedback control was also added. The process values were turbidity and suspended solids. The study assumed feedback control parameters were measured immediately after dosing coagulant, and thus took no consideration to hydraulic retention time. The result showed that combining feedforward and feedback improved model qualities for dosage adjustment, which made effluent concentration more stable. Coagulant dosage for the WWTP was reduced by 9 %.

## 2.6 Controller tuning approach - The Lambda method

The Lambda method is commonly used to calibrate regulators. The method consists of four steps and is described by SvensktVatten (2010c). The process for tuning a PI regulator is outlined below.

1. Change of setpoint value.
2. Measure the step response from the process value,  $\Delta y$ , and note time for step response change.
3. Calculate lambda,  $\lambda$ .
4. Calculate control parameters for the regulator, based on the Lambda value.

The regulator should be disconnected at step 1. The change of setpoint value should be swift and the amplitude,  $\Delta u$ , saved. At step 2, the time it takes for the process value to reach 63% of the setpoint is noted as T, figure 9 . Any possible dead time, L, should also be noted. The process gain,  $K_P$ , is calculated as in equation 25.

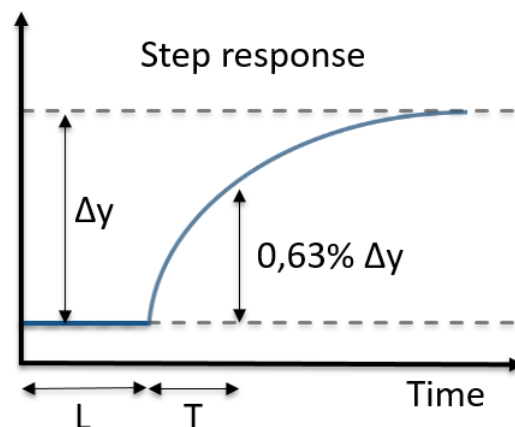


Figure 9: Parameters used in the Lambda method.

$$K_P = \frac{\Delta y}{\Delta u} \quad (25)$$

In step 3, lambda is calculated according to equation 26.  $p$  should be adjusted to fit the process. A low value,  $<1$ , will result in a swift regulation whereas a high value,  $>3$ , will lead to a slow but stable regulation. Common values for  $p$  are between 2 and 3.

$$\lambda = p \cdot T \quad (26)$$

Control parameters calculated at step four are control gain,  $K_{FB}$  and  $T_I$  according to equation 27 & 28. The control parameters are starting values, and can if needed further be fine-tuned.

$$K_{FB} = \frac{T}{K_P(\lambda + L)} \quad (27)$$

$$T_I = T \quad (28)$$

### 3 Background

This section contains the performed national analyses. The section also describes Tivoli WWTP, and Tivoli's issue with irregular load deriving from Regnbågen.

#### 3.1 National analysis: Experiences from other WWTPs

Experiences from other WWTPs were gained by contacting several municipal corporations with a questionnaire. The questions asked in the questionnaire are shown below.

1. *How many PE<sup>2</sup> is the WWTP designed for, and what is the current load?*
2. *What is maximum designed influent flow rate, and what is the average influent flow rate?*
3. *What is the wastewater treatment process? Is pre-precipitation, simultaneous precipitation or post-precipitation used?*
4. *What coagulants are used for chemical precipitation?*
5. *Which control strategy is used for chemical precipitation?*
6. *Does the control strategy give satisfactory results?*

A summary of the questionnaire is seen in table 3. The full overview is seen in appendix A. From table 3 it is clear that both the placement of the chemical treatment and control strategy varies much within Sweden. All WWTPs expect Kungsängsverket were satisfied with their control strategy, who are having issues with post-precipitation. Both Öns WWTP and Himmerfjärdsverket uses pre-precipitation and face challenges with their control strategy during high flows. Öns WWTP uses feedforward proportional to TSS, which is the same control strategy as Tivoli currently has.

---

<sup>2</sup>PE stands for population equivalent and is organically degradable material. 1 PE equals 70 grams of BOD7, biochemical oxygen demand for 7 days (Naturvårdsverket, 2017).

Table 3: Chemical treatment and control strategies of WWTPs within Sweden. Chemical treatment and control strategies within parenthesis are used occasionally.

Treatment plant <i>Organisation and/or city</i>	Chemical treatment	Control strategy	Satisfactory results?
- Tivoli <i>MittSverige Vatten &amp; Avfall Sundsvall</i>	pre-precipitation	feedforward: SS and time proportional	No
- Simsholmen <i>Tekniska kontoret, Jönköping</i>	pre-precipitation	time proportional	yes
- Kungsängsverket <i>UppsalaVatten</i>	pre-precipitation post-precipitation (simultaneous precipitation)	feedforward: flow feedforward: phosphate <sup>3</sup> (feedforward: flow)	yes no <sup>4</sup> -
- Ryaverket <i>Gryvabb, Göteborg</i>	simultaneous precipitation (direct precipitation)	feedback: phosphate (feedback: SS & flow)	yes yes
- Öns WWTP <i>Vakin, Umeå</i>	pre-precipitation post-precipitation	feedforward: SS feedback: flow	yes <sup>5</sup> yes
- Käppalaverket <i>Käppalaförbundet, Stockholm</i>	simultaneous precipitation post-precipitation (direct precipitation) <sup>6</sup>	feedback: phosphorous feedback: phosphate -	yes yes -
- Himmerfjärdsverket <i>Syovab, Stockholm</i>	pre-precipitation	feedforward: flow and feedback: SS & phosphate	yes <sup>7</sup>
- Göviken <i>Östersunds kommun</i>	pre-precipitation  (post-precipitation)	feedforward: TS and feedback: flow -	yes
- Henriksdals WWTP <i>Stockholm Vatten &amp; Avfall</i>	pre/simultaneous precipitation <sup>8</sup> post-precipitation	time proportional feedback: phosphate	yes yes
- Bromma reningsverk <i>Stockholm Vatten &amp; Avfall</i>	pre/simultaneous precipitation <sup>9</sup> (summer) (post-precipitation)	still testing feedforward: flow (feedback: phosphate) <sup>10</sup>	- yes -

<sup>3</sup>Incoming phosphate concentration to the chemical treatment.

<sup>4</sup>Low total organic carbon create challenges for this precipitation, and the process can be optimised. Today, coagulant is overdosed.

<sup>5</sup>Works well under normal circumstances. During extreme high flows, the dosage must be adjusted.

<sup>6</sup>Uses Actiflo, which is a more affective than conventionall direct precipitation. Actiflo improves settling by add polymers, micro sand followed by a lamell discs (Sweco , 2013).

<sup>7</sup>Works well under normal circumstances but need much manual control under high flows.

<sup>8</sup>Coagulant is dosed at inlet of the WWTP, but is not oxidised before the biological treatment. Therefore it works as a simultaneous precipitation.

<sup>9</sup>Coagulant is dosed at inlet of the WWTP, but is not oxidised before the biological treatment. Therefore it works as a simultaneous precipitation.

<sup>10</sup>With restriction deriving from flow.

## 3.2 Tivoli WWTP

Tivoli WWTP is the largest WWTP in Sundsvall and currently receives a load of 50 000 PE and has an average influent flow rate of 23 000 m<sup>3</sup>/day. Tivoli is designed for up to 85 000 PE and a maximum influent flow rate of 26 400 m<sup>3</sup>/day. Tivoli started operating in 1970 and is build inside of Norra Berget, a mountain north of Sundsvalls city. The treated effluent from Tivoli is released into Sundsvallsbukten (MSVA , 2020). Tivoli's wastewater treatment process is seen in figure 10.

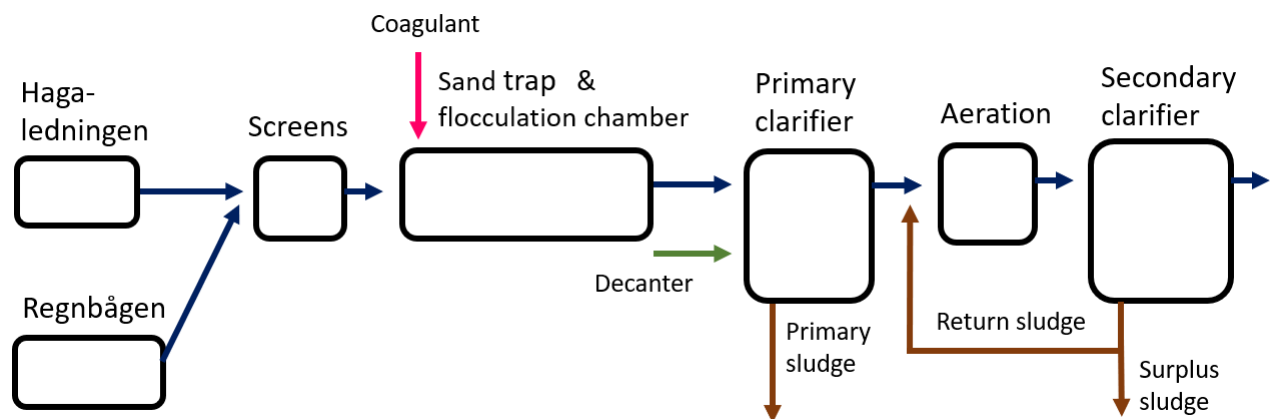


Figure 10: Overview of Tivoli WWTP.

The wastewater enter Tivoli WWTP either from Haga-ledningen or from an equalisation tank, Regnbågen. About one fifth of the wastewater originates from Haga-ledningen, which is an upstream sewer network. The rest of the wastewater is first upheld in Regnbågen. Tivoli has two parallel precipitation lines between the screens up to the secondary clarifier, where the wastewater is distributed over four clarifiers. The coagulant is added at the inlet of the sand trap. The outflow from the decanter is added to one of the primary clarifiers. The decanter originates from a sludge thickener (Malovanyy , 2015) .

### 3.2.1 Purpose and problems with the equalisation tank

Regnbågen is a later extension to Tivoli, and was built in 1990 to avoid overloading that were a result of combined pipes for storm- and drainage water in the sewage system. During storm weather and snow melting the combined pipes resulted in flows that exceeded Tivoli's wastewater treatment capacity. Regnbågen consists of a 2 km long tunnel inside of Norra Berget and holds 30 000 m<sup>3</sup>. Wastewater is pumped 5-25 m up from Regnbågen to Tivoli WWTP, depending on the current water level inside the tank.

Although Regnbågen successfully avoids overloading since its installation, the equalisation changes the pollutant dynamics of incoming wastewater. Typically, incoming load is mirrored by societies activities, and there is a good correlation between incoming phosphate and suspended solids. Sand, sludge and suspended solids present in the wastewater in Regnbågen settles, due to the wastewater slow flow rate inside Regnbågen. The settled matter is removed 1-2 times a day, by reducing the water level in Regnbågen and pump the settled matter to Tivoli WWTP. Reducing the water level

in Regnbågen cannot be done during periods with high flow, which results in an accumulation of settled material in Regnbågen. When the water level in Regnbågen is reduced, incoming particulate load to Tivoli increases rapidly as the settled matter is pumped to Tivoli. Incoming suspended material is therefore more dependent on the water level in Regnbågen, than on societies activities <sup>11</sup>.

### 3.2.2 Current control strategy

The coagulant used at Tivoli is PAX, which is an aluminium based coagulant. The dosing of PAX is currently regulated by feedforward control proportional to incoming concentration of suspended solids. Tivoli additionally uses a time-based control. During daytime between 08:00-16:00, more coagulant is dosed per kg suspended solids than during nighttime. The dosing of PAX is also adjusted to the water level in Regnbågen. The water level can be divided into a top layer, which is the standard level, middle and bottom layer. During the standard water level, no extra coagulant is added. When the water level in Regnbågen is reduced, the water level is cut to middle- and bottom layer. During the emptying, extra coagulant is dosed in order to achieve sufficient cleaning due to higher loads of particulate matter present in the lower layers. The extra dose of coagulant is higher when water is pumped from the bottom level than from the middle layer.

Tivoli used to regulate the coagulant dosage by feedforward control proportional to incoming soluble phosphate, with good results. However, the phosphate sensor was quickly polluted by incoming wastewater. This created difficulties to keep the sensor clean and the control strategy was therefore changed to proportional to suspended solids, as sensors measuring suspended solids are less sensitive.

### 3.2.3 Tivoli's issue with irregular load

The current control strategy significantly increases the coagulant dosage during the emptying of Regnbågen, in order to compensate for the extra incoming load. A high dosage of coagulant can result in the precipitation of phosphate being too high, which will deteriorate the growth of bacteria during aeration. Consequences of this are far-reaching, as it makes the bacteria composition less diverse and therefore negatively effect the biological treatment step. At the same time, if load peaks are not addressed with the right chemical dosage effluent concentration of phosphate will be too high.

Tivoli uses pre-precipitation and lacks consequently ability to reduce the phosphate concentration after the biological treatment. It is therefore extra important, that the precipitation of phosphorus works to satisfaction.

## 4 Method

This section describes first sampling of data, followed by model calibration of ASM2d and the primary clarifier model. Next, the construction of the soft sensor is described followed by the development of the control strategies. Lastly, the upbringing of a multicriteria-analysis is described.

---

<sup>11</sup>Malin Tuveesson, personal communication.

## 4.1 Sampling of data

### 4.1.1 Data measurements

Data for this project consists of both lab measurements and online data. Table 4 lists all measurements used in this project, and figure 11 shows where in Tivoli the measurements were taken. Online data is shown above the blue line in figure 11, and lab measurements under the same line.

Table 4: Data measurements. Filtered phosphate of online data is denoted as  $\text{PO}_4\text{-P}^{**}$  and lab measurements are denoted as  $\text{PO}_4\text{-P}^*$ .

Online data			Lab measurements		
Index	Measurement	Unit	Index	Measurement	Unit
H	Height of wastewater in Regnbågen	[m]	Con	Conductivity	[S/m]
T	Temperature	[°C]	$\text{PO}_4\text{-P}$	Phosphate	[mg/l]
$Q_W$	Waterflow	[m <sup>3</sup> /h]	$\text{PO}_4\text{-P}^*$	Filtered phosphate through 1.2 $\mu\text{m}$	[mg/l]
pH	pH	$-\log[\text{H}^+]$			
SS	Suspended solids	[mg/l]			
$Q_C$	Coagulantflow	[l/h]			
$\text{PO}_4\text{-P}^{**}$	Filtered phosphate through 0.45 $\mu\text{m}$	[mg/l]			
$Q_{PS}$	Primary sludgeflow	[m <sup>3</sup> /h]			
$\text{TS}_{PS}$	Total solids in primary sludge	[%]			

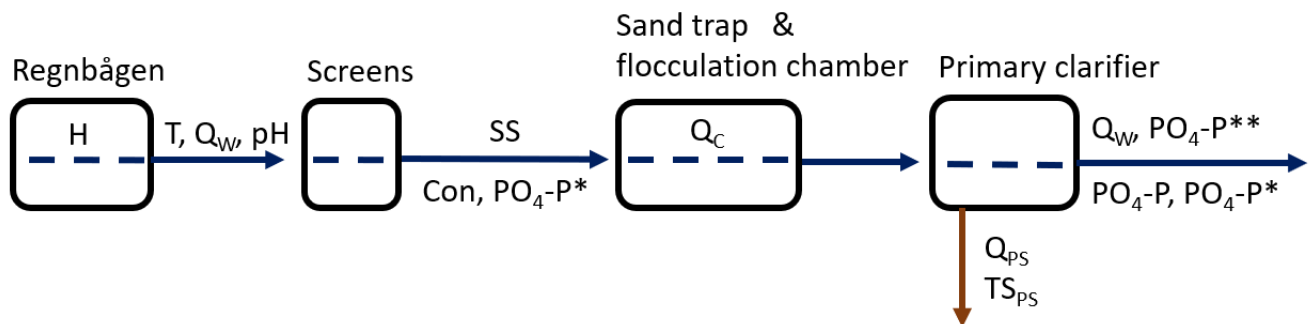


Figure 11: Measurements taken at Tivoli.

Online data is continuously measured by sensors. The data was collected from aCurve<sup>12</sup> with the time resolution of one hour. Lab measurements were sampled by two carousel samplers, the first placed after the screens and the second after the primary clarifier. The carousel samplers were set to fill a bottle with wastewater at predetermined intervals. The wastewater was analysed around 08:00 each morning, which means that wastewater could stand up to 24 hours in the bottle.

<sup>12</sup>A program used at Tivoli for monitoring and analysing online data.

Phosphorus measurements were analysed at an accredited lab by staff. The pore size of filters used in the lab are 1.2  $\mu\text{m}$ , and filtered phosphate values from the lab can thus be considered dissolved. The filtered phosphate measured by the sensor has a pore size of 0.45  $\mu\text{m}$ . It was believed that the difference in pore filter size would have no impact on effluent phosphate concentration from the primary clarifier, and thus that  $\text{PO}_4\text{-P}^{**}$  would be mirrored by  $\text{PO}_4\text{-P}^*$ .

Conductivity was measured directly at Tivoli using a multi-sensor. The sensor measures conductivity both with and without temperature correction. Conductivity with temperature corrections was used in calculations, as the wastewater had time to warm/cool before it was analysed.

At Tivoli suspended solids, SS, and total solids, TS, are measured. The model simulates total suspended solids, TSS. In this thesis, TS and TSS are assumed to be equivalent.

#### 4.1.2 Sampling campaign

The sampling campaign took place between the 15th and 19th of March. Data measurements for conductivity, incoming lab filtered phosphate,  $\text{PO}_4\text{-P}^*$ , and effluent phosphate,  $\text{PO}_4\text{-P}$ , was sampled every second hour from 00:00 on the 15:th to 08:00 on the 19:th of March. To confirm that effluent phosphate measured by the sensor,  $\text{PO}_4\text{-P}^{**}$ , was mirrored by lab measurements,  $\text{PO}_4\text{-P}^*$ , six samples of  $\text{PO}_4\text{-P}^*$  effluent from the primary clarifier were sampled. However, the assumption that pore filter size would have no impact on effluent phosphate concentration proved to be false. This created complications in the calibration of ASM2d, as  $\text{PO}_4\text{-P}^*$  is the incoming concentration to the primary clarifier but there were no continuous measurements of effluent  $\text{PO}_4\text{-P}^*$  from the clarifier. This is further discussed in section 4.2.3.2 *Determine phosphate concentration to calibrate ASM2d by*.

For the construction of the soft sensor, additional measurements were taken to validate the correlation between incoming soluble phosphate and other characteristics in incoming wastewater. The sampling of validation data was taken every third hour from 00:00 on the 22:nd to 00:00 the 23:rd of March.

Two complications appeared during the sampling campaign. The first happened on the 16:th at 14:00, when the carousel sampler containing incoming wastewater missed to fill the bottle. No lab measurements was therefore collected for incoming wastewater at this time. The second happened on the 15:th between 13:00 to 14:00, when the electricity had a breakdown. Therefore, no online data was collected during this time.

Furthermore, two circumstances appeared that might have influenced the results. On the 16:th between 14:00 to 16:00, measurements for flow rate was reduced to zero and shortly afterwards increased to twice the typical flow rate. These measurements were considered to be outliers and were deleted. Coagulant flow also had similar deviating values and were considered as outliers. Lastly, between the 15:th to the 17:th only one of the sand traps, where the flocculation occurs, was in use. This increases the flow rate and thus shortens time for flocculation. Both primary clarifiers were in use.

## 4.2 Model calibration

ASM2d and the primary clarifier model were calibrated according to Tivoli's conditions. This was done by 1) characterise influent parameters, 2) adjust ASM2d to an aluminium based coagulant and calibrate model parameters, 3) adjust the primary clarifier model to an aluminium based coagulant and calibrate model parameters.

### 4.2.1 Influent characterisation

Influent characterisation parameters to the model consists of state variables, table 2, and two additional parameters; flow rate and temperature. Henze, et. al. (2002) has proposed literature values for the state variables, but the model provided had default values that varied slightly. The parameters for the influent characterisation measured in this project are soluble phosphate, which is filtered phosphate,  $PO_4-P^*$ , particulate material<sup>13</sup>, flow rate and temperature. The parameters that are not measured were estimated by the standard influent characterisation used in BSM2. The parameters were therefore estimated by running the simulation in steady state with the models default values, but with updated values for the measured parameters. Mean values used for the simulation of the measured parameters are seen in table 5. The simulation saved new values for the state variables, which were used as influent characterisation further on.

Table 5: Measured parameters for influent characterisation.

Parameter		Tivoli mean value	Unit
Soluble phosphate	$S_{PO_4-P^*}$	2.2	gP $^{-3}$
Particulate material	$X_{TSS}$	250	gTSS $m^{-3}$
Flow rate	$Q_W$	23 000	$m^3/day$
Temperature	T	8.9	$^{\circ}C$

Prior to running the simulation the flow rate was converted from [ $m^3/h$ ] to [ $m^3/day$ ], which is the required unit set by the model. Additionally, the volume of the primary clarifier been updated according to the size of Tivoli's primary clarifier.

For dynamic influent data the model requires a measurement every 15:th minute. Since both lab and online data had a wider time resolution, dynamic influent data was interpolated. The interpolation for online data is shown appendix B, figure 1, and measured lab data with the interpolation is shown in appendix B figure 2.

### 4.2.2 Addition of coagulant

The main coagulant dosage characteristics required for modelling are coagulant flow rate, concentration of aluminium hydroxide,  $Al(OH)_3$  within the coagulant, and concentration inorganic suspended solids, ISS, within the coagulant. For the calibration

<sup>13</sup>Particulate material is the concentration of total suspended solids, consisting of measured suspended solids in the wastewater and of particulate matter from the coagulant.

of ASM2d and the primary clarifier model, the measured coagulant flow rate was converted into [m<sup>3</sup>/day].

The concentration of aluminium hydroxide was calculated by first finding the mass of aluminium dosed per cubic meter PAX, and use stoichiometry to find the concentration of aluminium hydroxide, equation 29 - 31.

$$m_{Al} = v_{PAX} * \rho_{PAX} * Al_{Procent} \quad (29)$$

$$n_{Al(OH)_3} = n_{Al} = \frac{m_{Al}}{M_{Al}} \quad (30)$$

$$c_{Al(OH)_3} = \frac{m_{Al(OH)_3}}{v_{PAX}} = \frac{M_{Al(OH)_3} * n_{Al(OH)_3}}{v_{PAX}} \quad (31)$$

In the equations are m=mass [g], v=volume [m<sup>3</sup>],  $\rho_{PAX}$  = density of PAX [g/m<sup>3</sup>],  $Al_{Procent}$ = percent weight of aluminium in PAX, n=mol, M=molar weight [g/mol] and c=concentration [g/m<sup>3</sup>].

The concentration of ISS was assumed to be equal to the concentration of aluminium hydroxide, according to equation 32.

$$c_{ISS} = c_{Al(OH)_3} \quad (32)$$

### 4.2.3 ASM2d model

#### 4.2.3.1 Adjust stoichiometric coefficients for aluminium based precipitation

ASM2d was calibrated after an aluminium based coagulant using stoichiometry coefficients for aluminium hydroxide and aluminium phosphate,  $AlPO_4$ , table 6. This enables ASM2d to calculate the process rate of precipitation and redissolution, according to equation 7 & 8.

Table 6: Stoichiometry of precipitation and redissolution of phosphate. It is shown how many grams of  $X_{Al(OH)_3}$ ,  $X_{AlP_3}$  and  $X_{TSS}$  that is reduced or formed when 1 g  $S_{PO_4P}$  is precipitated/redissolved.

Process	$S_{PO_4}$	$X_{Al(OH)_3}$	$X_{AlPO_4}$	$X_{TSS}$
Precipitation	-1	-2.52	3.94	1.42
Redissolution	1	2.52	-3.94	-1.42

$S_{PO_4P}$ ,  $X_{Al(OH)_3}$  and  $X_{AlPO_4}$  are the compounds molar weight divided by the molar weight of phosphate. Equation 33 & 34 shows the calculation of  $X_{Al(OH)_3}$ ,  $X_{AlPO_4}$  and  $S_{PO_4}$  were calculated similarly. For  $S_{PO_4}$ , only the phosphorus atom is included in the molar weight because ASM2d is set to calculate phosphate in [gP/ m<sup>3</sup>], instead of [g $PO_4$ -P/ m<sup>3</sup>].  $X_{TSS}$  is the absolute value difference between  $X_{Al(OH)_3}$  and  $X_{AlPO_4}$ .

$$M(Al(OH)_3) = M(Al) + 3 \cdot M(OH) = 26.98 + 3 \cdot (16 + 1.008) = 78.004 \quad (33)$$

$$X(Al(OH)_3) = \frac{M(Al(OH)_3)}{M(P)} = \frac{78.004}{30.97} = 2.52 \quad (34)$$

#### 4.2.3.2 Determine phosphate concentration to calibrate ASM2d by

Input phosphate concentration to the model is incoming lab filtered phosphate, PO<sub>4</sub>-P\*. Figure 12 shows all measured effluent phosphate concentrations. As it was believed that PO<sub>4</sub>-P\* and PO<sub>4</sub>-P\*\* would mirror each other, the plan had been to calibrate ASM2d after the sensor. However, the sensor measured PO<sub>4</sub>-P\*\* to be significantly lower than the samples of lab filtered phosphate, PO<sub>4</sub>-P\*.

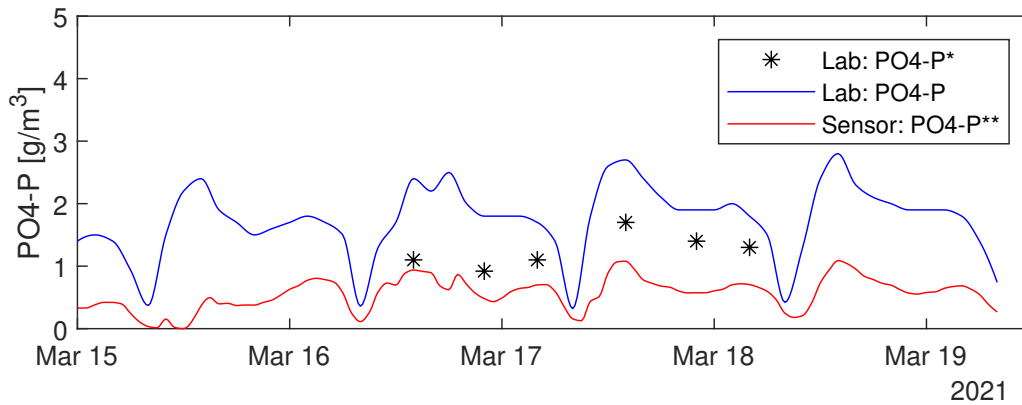


Figure 12: Measured effluent phosphate concentration from the primary clarifier.

This provided a complication, as it is desirable that the effluent concentration used to calibrate ASM2d by should correspond to the incoming concentration. It was therefore tested to estimate effluent PO<sub>4</sub>-P\* by using a historical fraction, which was calculated to 0.72. This historical fraction originates from a time when Tivoli used iron as coagulant and both phosphate and filtered phosphate was measured after the primary clarifier. The conformity of the estimated PO<sub>4</sub>-P\* by the historical fraction with measured PO<sub>4</sub>-P\* during the sampling campaign are shown in appendix D, figure 1. The historical fraction miss-predicted two of the six measurements considerably.

It was decided to calibrate ASM2d against the sensor measurements, PO<sub>4</sub>-P\*\*, as the historical fraction miss-predicted the effluent PO<sub>4</sub>-P\* concentration. Furthermore, it was in the interest of the staff to calibrate the ASM2d after the sensor as it is easy to implement in practice. However, when interpreting the model results, the difference between the filter pore size in input and effluent phosphate concentrations should be remembered.

#### 4.2.3.3 Rate constant for precipitation and redissolution

De Haas et. al. (2001) suggested values for K<sub>PRE</sub>, K<sub>RED</sub> and K<sub>ALK</sub>, defined in equation 7 & 8, for alum<sup>14</sup>. Attempts were made to calibrate ASM2d accordingly. However, the suggested values by De Haas et. al. (2001) resulted in too low precipitation. The rate constants were therefore significantly increased to receive a higher precipitation. Two promising combinations of values of the parameters are shown in table 7. The

<sup>14</sup>An aluminium sulphate that can be used as coagulant.

best alternative was determined by calculating the percentage difference between the models estimations of phosphate and the measured phosphate concentration.

Table 7: Tested combinations of values for  $K_{PRE}$ ,  $K_{RED}$  and  $K_{ALK}$ . Alternative 1 is suggested by De Haas et. al. (2001).

Combination of parameters	Kpre	Kred	Kalk	Percentage difference
Alternative 1	0.0006	0.00036	0.5	-206,2
Alternative 2	50	10	0.4	0.165
Alternative 3	100	60	0.5	-28.3

Alternative 2 had the smallest difference between the estimated phosphate concentration and the measured, and was judged to be the most promising combination of parameters. Alternative 2 is therefore used further on. However, an additional consequential error analysis was performed which compares alternative 2 and 3 performance of the modelled phosphate concentration for the optimal control strategy.

To investigate whether ASM2d's performance was affected by using  $PO_4\text{-P}^*$  as input parameter but calibrate ASM2d after  $PO_4\text{-P}^{**}$ , it was also tested to calibrate ASM2d after the historical fraction. Good values for rate constants were  $K_{PRE}=0.8$ ,  $K_{RED}=0.48$  and  $K_{ALK}=0.5$  when ASM2d was calibrated after the historical fraction.

## 4.2.4 Primary clarifier model

### 4.2.4.1 Adjust stoichiometric coefficients for aluminium based precipitation

The primary clarifier model was calibrated so the stoichiometric coefficients would match aluminium, equation 35. The equation calculates total incoming aluminium from the ASM2d module to the primary clarifier module. In the equation are  $Al(OH)_3$  and  $AlPO_4$  multiplied with the fraction of the molar weight of aluminium in aluminium hydroxide and aluminium phosphate. The total amount of incoming aluminium to the primary clarifier is seen in figure 13.

$$Al_{tot} = 0.35 \cdot Al(OH)_3 + 0.22 \cdot AlPO_4 \quad (35)$$

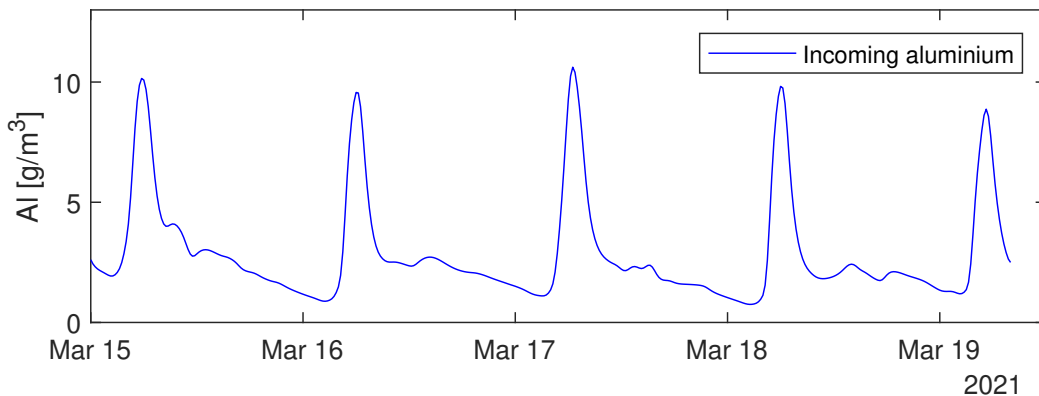


Figure 13: Total amount of incoming aluminium to the primary clarifier.

The total amount of aluminium present in the primary clarifier affects the settling. If the total amount of aluminium is low, the correction factor removal efficiency for aluminium,  $Al_{corr}$ , is low which leads to a poor settling and vice versa. There is a linear relationship between the lowest and highest  $Al_{corr}$  according to equation 36.  $Al_{tot.max}$  and  $Al_{tot.min}$  define limitations of the correction factor removal efficiency. If the current aluminium present in the primary clarifier is smaller than  $Al_{tot.min}$ , the correction factor removal efficiency is not lower than  $Al_{corr.min}$  and vice versa if the aluminium present is higher than  $Al_{tot.max}$ .

$$Al_{corr} = Al_{corr.min} + (Al_{tot} - Al_{corr.min}) \cdot \frac{Al_{corr.max} - Al_{corr.min}}{Al_{tot.max} - Al_{tot.min}} \quad (36)$$

An approximation of the maximum and minimum aluminium present in the primary clarifier was found through looking at figure 13, and suitable values for  $Al_{tot.max}$  and  $Al_{tot.min}$  could be determined.

Apart from the parameters in equation 36,  $f_{corr}$ ,  $f_x$  and  $f_{PS}$  defined in equation 13, 14 and 17 also had to be adjusted.  $f_{PS}$  is the proportional primary sludge flow rate to the influent flow rate, and could be calculated since both flow rates are measured. The other parameters could not be calculated, and different magnitudes of the values were tested. The default and selected values after calibration are shown in table 8.

Table 8: Calibration of the primary clarifier model.

Combination of parameters	$Al_{tot.min}$	$Al_{tot.max}$	$Al_{corr.min}$	$Al_{corr.max}$	$f_{corr}$	$f_x$	$f_{PS}$
Default	20	80	1	1.3	0.65	0.85	0.007
Selected	3	11	1	1.2	0.3	0.39	0.0063

The values were chosen after an iterative process, where one value was changed at a time. The performances of tested values were evaluated against mass balances, with the goal to minimise differences between modelled and estimated load of phosphate and total suspended solids. The mass balance of total suspended solids were also validated by adjusting modelled total suspended solids in the primary sludge against measured total solids, as a step in the iterative process.

#### 4.2.4.2 Mass balances

In order to receive reliable mass balances, a comparison over flow and a mass balance over modelled aluminium in the primary clarifier was conducted.

For the comparison over flow, figure 14, incoming flow to the primary clarifier was compared to total outgoing flow from the primary clarifier, for both measured and modelled flow. The total outgoing flow consists of the overflow from the primary clarifier and the flow of the primary sludge. The models estimation of total outgoing flow proved to be the exact same as measured incoming flow.

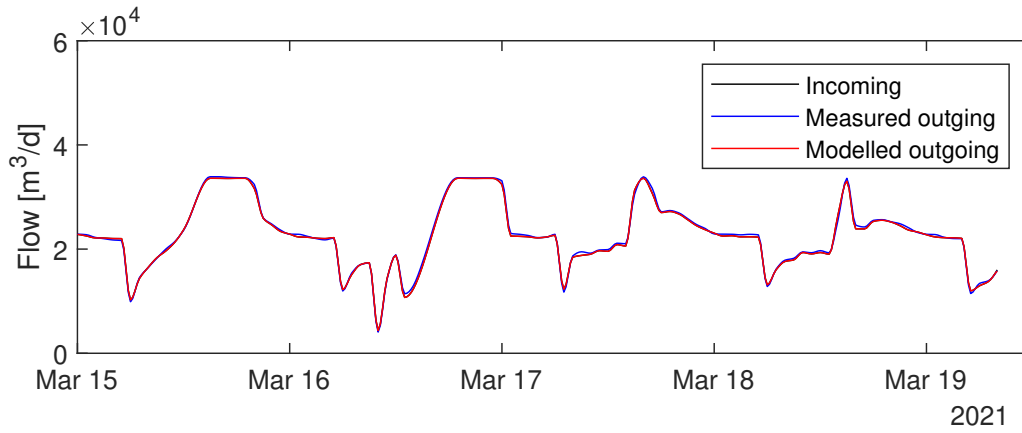


Figure 14: Comparison over flow.

The mass balance for aluminium were calculated according to equation 37 & 38, where  $l$ =load [g/day],  $c$ =concentration [g/m<sup>3</sup>] and  $q$ =flow [m<sup>3</sup>/day].

$$l_{inc} = c_{inc} \cdot q_{inc} \quad (37)$$

$$l_{out} = c_{out.Water} \cdot q_{out.Water} + c_{Sludge} \cdot q_{Sludge} \quad (38)$$

Incoming concentration was the state variables  $Me(OH)_3$  and  $MePO_4$  saved after the ASM2d module, and outgoing concentration was the same state variables saved after the primary clarifier module. Equation 35 was used to calculate the total amount of aluminium the in state variables. The mass balance for aluminium load is shown in figure 15. The percentage difference between incoming and outgoing load was roughly 1.2 %.

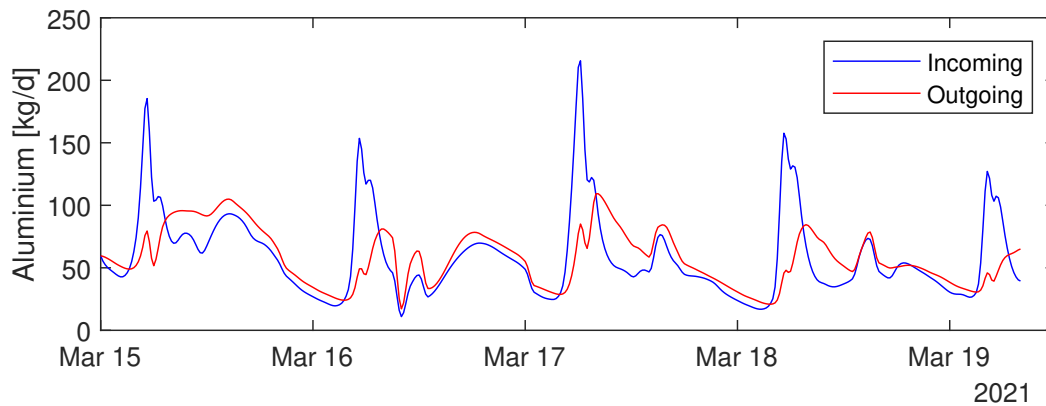


Figure 15: Mass balance for aluminium over the primary clarifier.

Equation 37 and 38 were also used to create mass balances for the load of soluble phosphate and total suspended solids. Incoming concentration for the mass balance over phosphate was  $PO_4-P^*$ . The models estimation of outgoing phosphate concentration was calculated by adding the state variables  $S_{PO_4}$  and contribution of phosphate in  $X_{MeP}$ . The concentration of phosphate within aluminium phosphate was calculated according to equation 39 where 0.25 is the molar weight fraction of phosphate.

$$C_p = 0.25 \cdot C_{AlP} \quad (39)$$

Incoming total suspended solids consists of measured suspended solids and the calculated contribution of aluminium hydroxide and inorganic suspended solids deriving from the coagulant. Outgoing total suspended solids is the models estimation of total suspended solids. The modelled load in the primary sludge was compared to and adjusted after measured total solids, figure 16. The concentration of measured total solids were estimated by assuming 1% = 10 000 [g/ton] according to SvensktVatten (2010d).

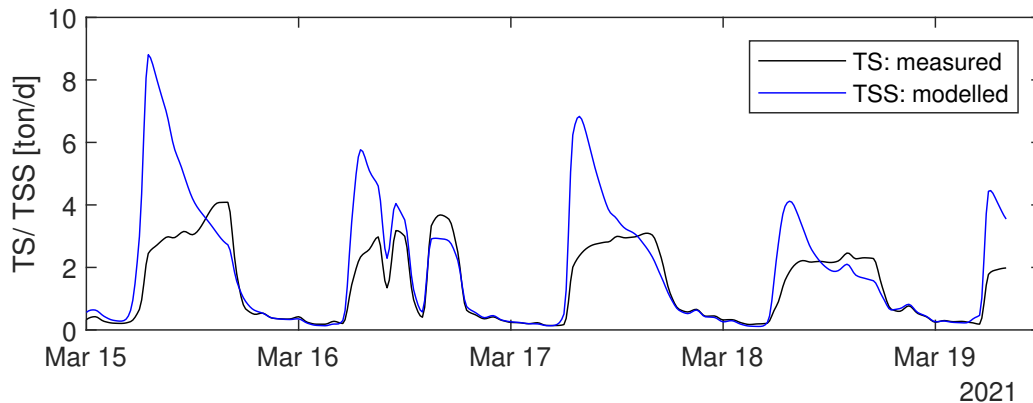


Figure 16: Measured and modelled load of total solids/ total suspended solids in primary sludge.

It was decided to not include the contributions from the decanter to the model. This was primarily done by two reasons. The first was that neither ASM2d or the primary clarifier model includes this contribution. The second reason was that the available data from the decanter was old, and therefore uncertain how much it resembled the current contribution of phosphate and suspended solids. The available data was analysed, and the contributions from the decanter were small in comparison with incoming load.

### 4.3 Prediction of phosphate

Incoming phosphate is hard to measure online (IVL , 2008), which creates challenges if feedforward control proportional to incoming phosphate is to be implemented at Tivoli. A soft sensor is a virtual sensor that can estimate parameters that are hard to measure online, by combining information from more easily measured parameters<sup>15</sup> (IVL , 2008). The original plan was to calibrate a soft sensor but due to lack of equipment not all easily measured parameters could be measured.

Instead, a simplified version of a soft sensor was created that didn't combine the information of the easily measured parameters. The constructed soft sensor only investigates the correlation between incoming phosphate and other incoming parameters individually. Regression lines were plotted showing the correlation of incoming filtered phosphate,  $PO_4\text{-P}^*$ , with incoming suspended solids, flow rate, temperature, pH,

<sup>15</sup>Easily measured parameters are needed for calibration of a soft sensor are flow, temperature, TSS, pH, conductivity and redox potential (IVL , 2008).

conductivity and the water level in Regnbågen. Data used for the construction of the simplified soft sensor were sampled between 15:th to the 19:th of March. The data had first been interpolated to 15 minutes long intervals, in order to enable the prediction to be used in dynamic simulations later on, see appendix B figure 1 and 2.

Suspended solids and pH had promising linear relationship with filtered phosphate, see appendix C, figure 1, and therefore attempts were made to find a linear equation. Outliers were deleted in order to improve the correlation. For suspended solids all values above 350 mg/l were considered outliers, and all values below 7 was considered outliers for pH. These limitations were motivated in order to improve the linear relationship. However, for suspended solids, the limit excluded all peaks which is not desirable, because it eliminated the effect of Regnbågen. The linear regression that estimates phosphate from suspended solids and pH is shown in figure 17.

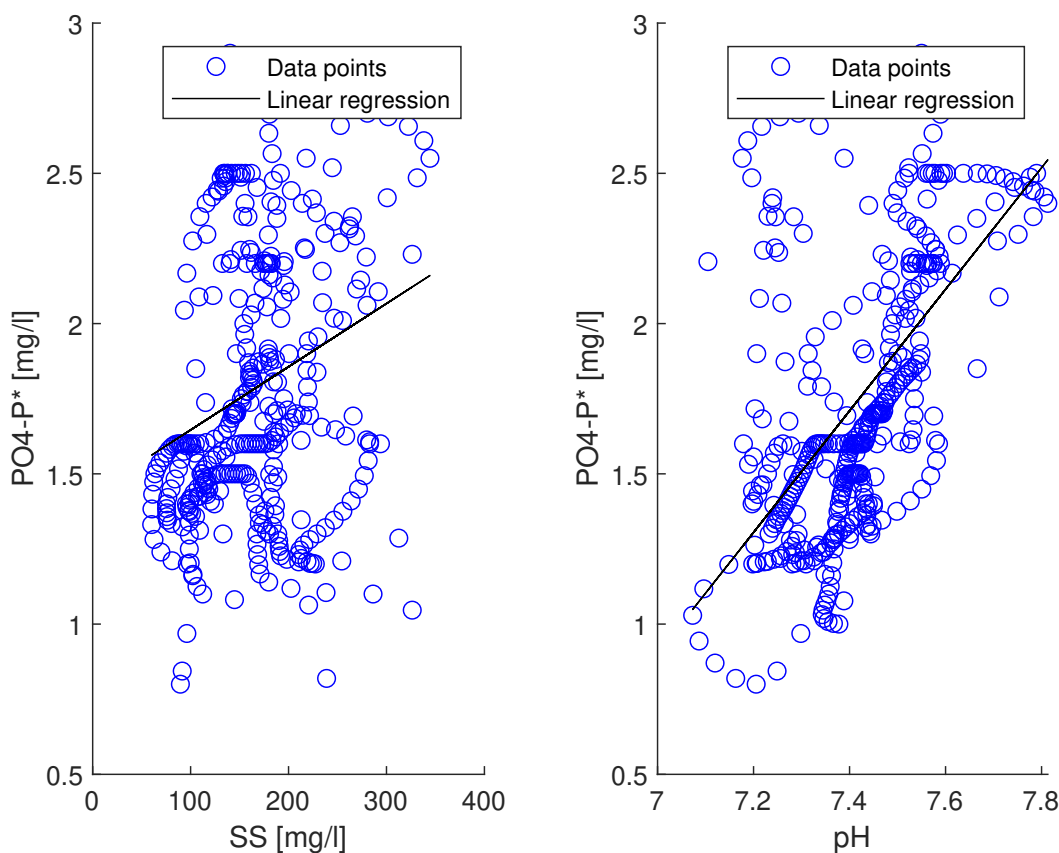


Figure 17: Linear regression for soluble phosphate plotted against suspended solids and pH.

The equation calculating phosphate from suspended solids had a  $r^2$  value of only 0.007, whereas the  $r^2$  value when pH was the independent variable proved to be higher, with a value of 0.377. Therefore, only pH was used to predict phosphate, according to equation 40.

$$\text{Phosphate concentration} = -13.2575 + 2.0226 \cdot pH \quad (40)$$

Calculating incoming phosphate from equation 40 gave negative phosphate values where  $pH < 7$ , which occurred between 00:00 and 08:00 on the 15:th, due to the limitations earlier drawn. Two paths were tested to overcome this. The first path was

simply not to view values  $\text{pH} < 7$  as outliers. However, this resulted in a much lower  $r^2$  value of 0.19. The second path was to compare what the measured incoming  $\text{PO}_4\text{-P}^*$  had been during the time when  $\text{pH}$  was below seven, and set the estimated phosphate concentration to a value close to the measured value. The second path was chosen, and all negative phosphate values were set to 1. This path was further motivated by examine the  $\text{pH}$  level during the past year, where  $\text{pH} < 7$  was observed roughly 3 % of the time.

To ensure that equation 40 not only works on calibration data, the equation was validated with measurements from the validation data, sampled the 22:nd and 23:rd of March. Additionally, consequential errors were analysed deriving from the miss-prediction of phosphate for feedforward control proportional to  $\text{pH}$ .

## 4.4 Control strategies

The control strategies; feedforward, feedback and feedforward combined with feedback are used to regulate the chemical dosage of the precipitant, and thereby effluent phosphate concentration. A reference value for effluent phosphate concentration from the primary clarifier was set to 0.76 [mg/l] according to the benchmark ratio for optimal bacteria growth. The reference value only considers the ratio between  $\text{BOD}_7$  and phosphate, as there is no continuous measurements for nitrogen. The calculated reference value is based on the mean value of  $\text{BOD}_7$  from one year prior the sampling campaign.

### 4.4.1 Feed forward

Three feedforward strategies were examined proportional to different disturbances. The strategies were:

- Feedforward based on the concentration of incoming suspended solids, FF: TSS.
- Feedforward based on incoming load of filtered phosphate, FF:  $\text{PO}_4\text{-P}$ .
- Feedforward based on incoming load of filtered phosphate, calculated using a soft sensor based on incoming  $\text{pH}$  measurements, FF:  $\text{pH}$ .

FF: TSS represents Tivoli's current control strategy. The flow of chemical dosage for FF: TSS was therefore measured, and could be used directly.

The coagulant flow for FF:  $\text{PO}_4\text{-P}$  and FF:  $\text{pH}$  were estimated by calculating the load of incoming phosphate, and using stoichiometry to find the mass of aluminium required to precipitate the incoming phosphate load. The theoretical stoichiometry between phosphate and aluminium is 1:1, as seen in equation 1. By using the weight percent of aluminium in PAX and the density of PAX, the required chemical dosage was found, equation 41 - 44.

$$l_P = c_P \cdot q_{\text{water}} \quad (41)$$

$$n_{Al} = n_P = \frac{l_P}{M_P} \quad (42)$$

$$l_{Al} = \frac{n_{Al}}{M_{Al}} \quad (43)$$

$$q_{PAX,T} = \frac{m_{PAX}}{\rho_{PAX}} = \frac{m_{Al}/Al_{procent}}{\rho_{PAX}} \quad (44)$$

In the equations are  $l$ =load [g/d],  $c$ =concentration[g/m<sup>3</sup>],  $q_{water}$ =flow rate of wastewater [m<sup>3</sup>/d],  $n$ =mol,  $M$ =molar weight [g/mol],  $Al_{percent}$ = weight present of aluminium in PAX,  $\rho$ =density of PAX [g/m<sup>3</sup>] and  $q_{PAX, T}$ = theoretical required chemical dosage to precipitate the incoming load of phosphate.

The calculated coagulant flow,  $q_{PAX, T}$ , is strictly theoretical and does not account for the precipitation calibrated in the model. To overcome this, incoming phosphate concentration was varied in steady state and effluent phosphate concentration analysed. The goal was to get the effluent concentration equal to the reference value. Seven variations of incoming phosphate were tested, from the minimum to the maximum phosphate concentration observed throughout the sampling campaign, table 9. The coagulant flow used for each simulation was calculated depending on incoming phosphate concentration, equation 41 - 44. Incoming phosphate concentration smaller than the mean concentration resulted in an effluent phosphate concentration lower than the reference value, and thus an overdose of coagulant. Incoming phosphate exceeding the mean value of phosphate also exceeded the reference value, and was therefore under-dosed. By multiplying the coagulant flow with a proportional gain for each simulation, the reference point for each effluent phosphate concentration was reached for all incoming concentration in steady state. This coagulant flow is denoted as  $q_{PAX, R}$ .

Table 9: Tested incoming phosphate concentrations in steady state. The percentage refers to the mean value of the phosphate concentration.

Phosphate concentration	Min	60%	80%	Mean value	120%	140%	Max
Proportional gain, $K_{FF}$	0.136	0.501	0.804	0.986	1.107	1.194	1.278

The relationship between  $q_{PAX, T}$  and  $q_{PAX, R}$  is described by the linear equation 45.

$$q_{PAX,R} = -0.25355 + 1.7129 \cdot q_{PAX,T} \quad (45)$$

Equation 45 was used to calculate the chemical dosage for dynamic simulations. However, this resulted in negative flows for a limited number of occasions. To avoid negative coagulant flows, all  $q_{PAX, R} < 0$  was set to 0. A comparison over  $q_{PAX, T}$  and  $q_{PAX, R}$  is seen in figure 45. It is seen that  $q_{PAX, R}$  follow the dynamic of  $q_{PAX, T}$ , but have more significant peaks.

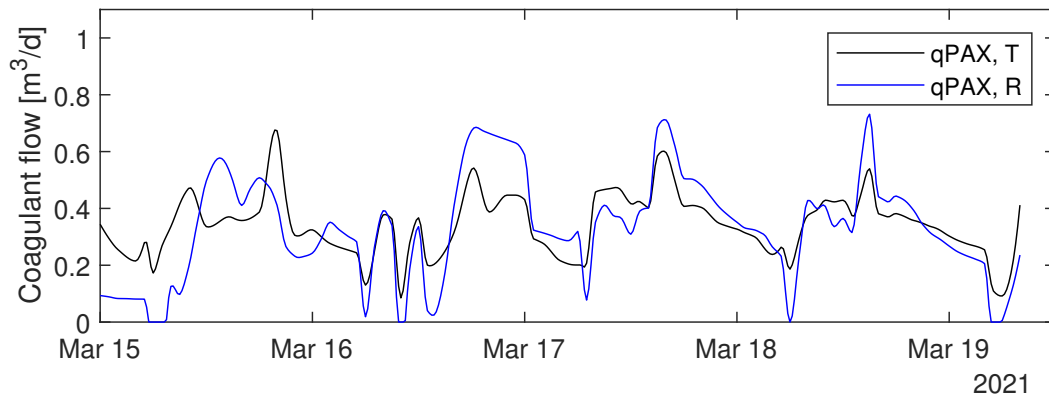


Figure 18: Theoretical,  $q_{PAX, T}$ , and adjusted coagulant flow to the reference value,  $q_{PAX, R}$ .

#### 4.4.2 Feedback

A loop was created from the primary clarifier module to the addition of coagulant, and within the loop was a feedback regulator added, figure 19. The control strategy for feedback control is denoted FB.

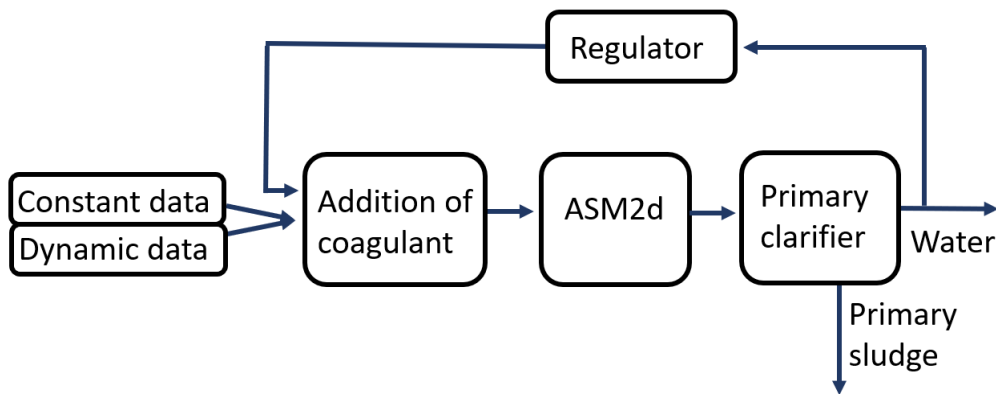


Figure 19: Simulink model for feedback control.

Incoming parameter to the feedback module is phosphate concentration, and outgoing parameter is the calculated flow rate of coagulant. An anti-windup was included in the regulator, which ensures that coagulant flow doesn't exceed chosen limits. The lower limit was set to zero, as a negative flow is not possible. The upper limit was set to 6  $[m^3/d]$ , a coagulant flow rate that is only exceeded twice in 1.5 years.

##### 4.4.2.1 Tuning the PI- controller

The control parameters for the PI- controller were calculated with the Lambda method. The change of setpoint correspond to a change in coagulant flow, and the step response in the process value is the phosphate concentration. The setpoints were set so the process values captured the reference point with  $\pm 0.5$ , table 10.

	Set point	Step response
Initial	0.318	0.81
After setpoint change	0.372	0.71

Table 10: Shows changes in setpoint, and corresponding change in process value.

At first, attempts were made with  $p=1-3$  but this resulted in a regulator that was too slow. Therefore, lower  $p$ -values were tested. Table 11 shows tested  $p$ -values and corresponding values for the process control parameters gain,  $K_{FB}$ .

Table 11: Tuning the PI-controller

Control parameter	$p=0.1$	$p=0.25$	$p=0.5$
$T_I$	0.1364	0.1364	0.1364
$K_{FB}$	-5.335	-2.1340	-1.067

Evaluation of the  $p$ -values was done by investigating the step response of the process value when the reference value was changed. In practice, the optimal phosphate concentration changes depending on the current benchmark ratio for bacteria growth. During the sampling campaign, the optimal phosphate concentration would be 0.81 mg/l. By changing the reference value from 0.81 to 0.76 (the optimal concentration of phosphate during the last year), the setting time and oscillation for the  $p$ -values could be seen. This is shown in figure 20. From the figure it is clear that oscillating behaviour increases when  $p$  is reduced. It is also seen that higher  $p$ -values result in slow changes, but little overshoot.

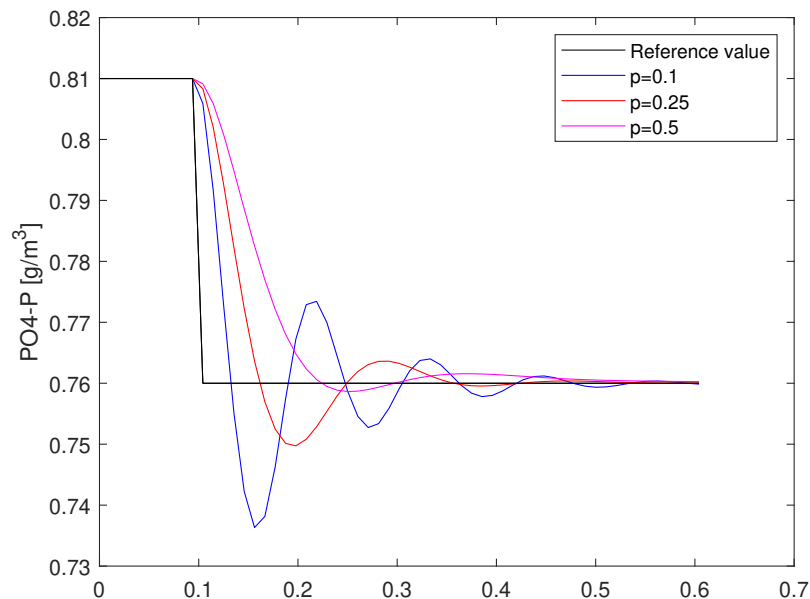


Figure 20: Change of reference value of phosphate concentration from 0.81 to 0.76.

It was judged that  $p=0.25$  was best suited. This is motivated by the phosphate reaches the new reference value the quickest. Furthermore, the change in reference value is 0.05, and the overshoot for  $p=0.25$  is roughly 0.011, which in comparison is small. Therefore is the risk low that an overshoot would have a significant negative affect on the biological treatment step.

#### 4.4.3 Feedback combined with feedforward

The combined feedforward and feedback control strategy was constructed by adding a summation block within the module *Addition of coagulant*. The anti-windup was kept within the regulator. The same disturbances were evaluated as for feedforward control. The combined feedforward and feedback control strategies are denoted FF & FB: TSS, FF & FB: PO<sub>4</sub>-P and FF & FB: pH.

A challenge with combining feedforward with feedback control is to find a good ratio of the contribution of feedforward and feedback respectively. Equation 46 estimates  $K_{FFFB}$  that determines how large the contribution of feedforward control should be.

$$K_{FFFB} = \frac{u1 - u2}{v1 - v2} \quad (46)$$

In the equation,  $u$  is the input signal, which corresponds to the coagulant flow, and  $v$  is a disturbance, in this case incoming phosphate to the primary clarifier.

The value received by equation 46 was  $K_{FFFB} = 0.34$ , which means that 34% of the dosage from feedforward control was used, and the contribution of feedback control made up the rest of the total dosage for the combined strategy. The calculated  $K_{FFFB}$  did not give satisfactory results and other values for  $K_{FFFB}$  were tested. The  $p$ -value chosen for the feedback regulator was low compared to values proposed by Svenskt-Vatten (2010c), which means the feedback regulator might be very swift. By combining feedforward with feedback, the  $p$ -value can sometimes be set to a higher value as the contribution of feedforward control allows feedback control to be slower<sup>16</sup>. Tested combinations of  $K_{FFFB}$  and  $p$  values are shown in table 12.

Table 12: Tuning the combined regulator.

Control parameter	$K_{FFFB}$	$p$
Option 1	0.34	0.25
Option 2	0.34	0.5
Option 3	0.7	0.25

There is a balancing act between the stability of outgoing phosphate concentration from the primary clarifier and swiftness of changes in coagulant flow. The phosphate concentration and coagulant flow was evaluated by running ASM2d and the primary clarifier model, for all three options. The feedforward contribution was proportional to measured incoming phosphate. Additionally, the contribution of feedforward and feedback control to the total chemical dosage was investigated for the best option.

<sup>16</sup>Bengt Carlson, personal communication.

## 4.5 Multi-criteria analysis

The control strategies were evaluated with a multi-criteria analysis. The criteria included the mean value of modelled phosphate concentration, the maximum variation in phosphate concentration, coagulant use, produced sludge and complexity, table 13. The criteria were weighted with a factor. Four intervals were created, and the performance of the control strategy determined in which interval the control strategy was placed in for each criteria. Points to the control strategies were determined by multiplying the index of the given interval with the factor for each criteria, and sum up the points. This way, control strategies placed in interval 4 for a certain criteria would receive higher points than a control strategy placed in interval 3. The control strategy with the highest points was viewed as the most promising.

Table 13: Weighting and intervals for the criteria in multi-criteria analysis.

Variable	Factor	Interval			
		1	2	3	4
Mean value PO <sub>4</sub> -P	0.3	± > 0.05	±0.03 → 0.05	±0.01 → 0.03	± < 0.01
Max. variation	0.2	>0.94	0.66→ 0.94	0.39→ 0.66	<0.39
Coagulant dosage	0.25	> 642	534→ 642	425→ 534	<425
Produced sludge	0.1	>506	504→ 506	502→ 504	<502
Complexity	0.15	FF + FB	FB	FF	Current

The intervals for mean value of phosphate were determined with regard to the reference value. The closer the mean value of phosphate was to the reference value, the higher interval would be control strategy be allocated in. The intervals limits are chosen so an equal distribution between the performance of the control strategies would be allocated.

The maximum variation in phosphate concentration is the difference between the highest and lowest modelled phosphate value. Coagulant dosage is consumed PAX in [kg/d], and produced sludge is produced primary sludge in [ton/d]. The intervals of the criteria span, coagulant dosage and produced sludge are calculated according to equation 47, where X is the index of the calculated interval.

$$IntervalX = Criteria_{min} + X \cdot \frac{Criteria_{max} - Criteria_{min}}{4} \quad (47)$$

The interval's for complexity were based on how hard the control strategy would be to implement in practice. The current control strategy would be the easiest to continue to practice, and was therefore placed in interval four. To combined control strategy is the most complex strategy, and was therefore allocated in interval 1.

## 5 Results and discussion

This section presents both results and associated discussion. Results from the model calibration of ASM2d and the primary clarifier model, the performance of the soft sensor and tuning of the combined control strategy is presented first. The subsection is followed by the results of the combined control strategy and the multi-criteria analyses. Next, consequential errors are pinpointed from the prediction of phosphate and choice of model parameters for ASM2d. The section is concluded with some general comments of improvements and uncertainties.

### 5.1 Model calibration

#### 5.1.1 ASM2d

The result from the calibration of ASM2d is shown in figure 21. It was decided to calibrate ASM2d after alternative 2, as the percentage difference between estimated and measured phosphate is only 0.165 %. The ASM2d estimation follows the dynamic of the measured phosphate concentration decently, and the estimation does not capture peaks. It also does not follow the measured phosphate as well as expected with respect to the low percentage difference. It can therefore be concluded that the estimation, almost equally, overestimates and underestimates the measured concentration. The model estimation for alternative 1 and 3 are seen in appendix D, figure 2.

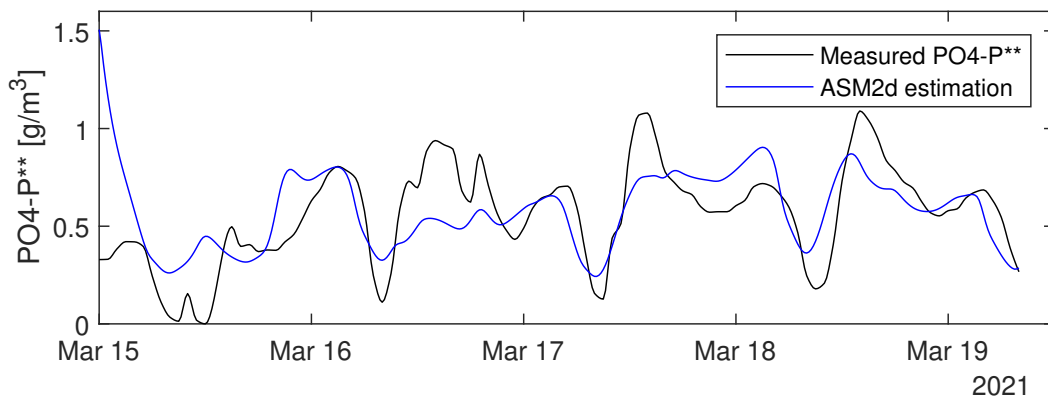


Figure 21: Outgoing phosphate concentration from the primary clarifier, calibrated against the sensor.

The decision to calibrate ASM2d after phosphate measured by the sensor,  $\text{PO}_4\text{-P}^{**}$ , even though  $\text{PO}_4\text{-P}^*$  does not comprehend with phosphate measured by the lab,  $\text{PO}_4\text{-P}^*$ , as seen in figure 12, had several consequences. The first complication is seen in figure 21, where the swift drop at the beginning of the simulation likely is due to the mismatch between input parameter, incoming  $\text{PO}_4\text{-P}^*$  to the primary clarifier, and what the model is calibrated after, outgoing  $\text{PO}_4\text{-P}^{**}$  from the primary clarifier. Additionally, it was required to significantly increase the rate constants for precipitation and redissolution,  $K_{\text{pre}}$  and  $K_{\text{red}}$ , proposed by De Haas et. al. (2001) in order to for the estimation of phosphate to match the magnitude of sensor measured phosphate. This is clearly seen in appendix D, figure 2, where alternative 1 resembles values proposed by De Haas et. al. (2001).

If the model instead was to be calibrated after the historical fractions estimate of  $\text{PO}_4\text{-P}^*$ , figure 22, the swift drop in the estimation of phosphate would disappear. However, the estimation would completely miss the frequent occurring dips in late morning. These dips derive from the measured phosphate,  $\text{PO}_4\text{-P}$ , which the historical fraction used to estimate filtered phosphate. As seen in figure 12, the dips occur for both  $\text{PO}_4\text{-P}$  and  $\text{PO}_4\text{-P}^{**}$ , but are much more significant for  $\text{PO}_4\text{-P}$ . It is therefore likely that the dips are amplified in the estimation of filtered phosphate,  $\text{PO}_4\text{-P}^*$ . If filtered phosphate outgoing from the primary clarifier had been measured frequently during the sampling campaign, the dips would likely be reduced which might have resulted in the best model estimation of phosphate.

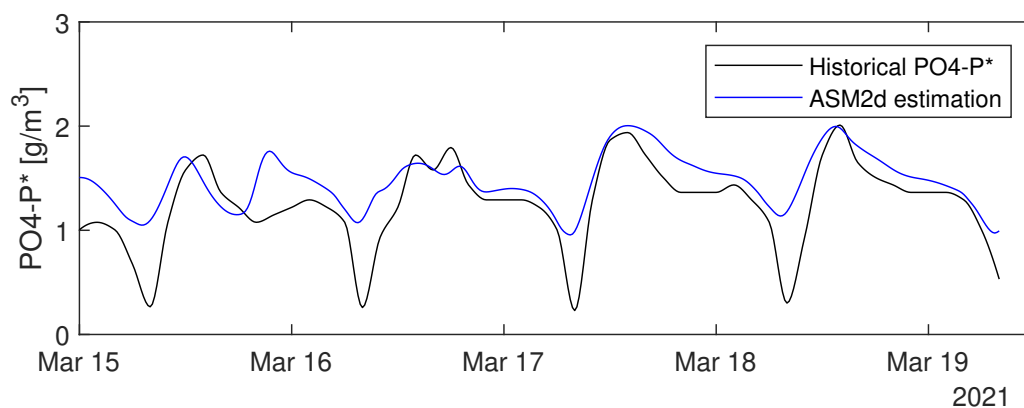


Figure 22: Outgoing phosphate concentration from the primary clarifier, calibrated against the historical fraction.

Calibrating ASM2d after the historical fraction resulted in  $K_{\text{pre}}$  to be increased from 0.0006 (proposed by De Haas et. al. (2001)) to 0.8. Calibrating ASM2d after the sensor ( $\text{PO}_4\text{-P}^{**}$ ),  $K_{\text{pre}}$  was set to 50. To calibrate the model after  $\text{PO}_4\text{-P}^*$  would stray less from earlier studies, which would have been preferable. By increasing the ratio between  $K_{\text{pre}}$  and  $K_{\text{red}}$ , an even lower  $K_{\text{pre}}$  value than 0.8 could most likely be achieved.

### 5.1.2 Primary clarifier model

Result of the calibration of the mass balances are seen in figure 23 and 24. The load percentage difference for phosphate is 0.69%, and 17.0% for total suspended solids. Modelled outgoing phosphate load nicely follows the measured incoming load. The conformity between modelled and measured load for total suspended solids is weaker. Measured suspended solids have sharp, high peaks deriving from the emptying of Regnbågen. The model acknowledged these peaks, but not to the same extent. The modelled peaks are also delayed and tends to linger. This is probably due to that the settling of matter depends on size of the flocs created.

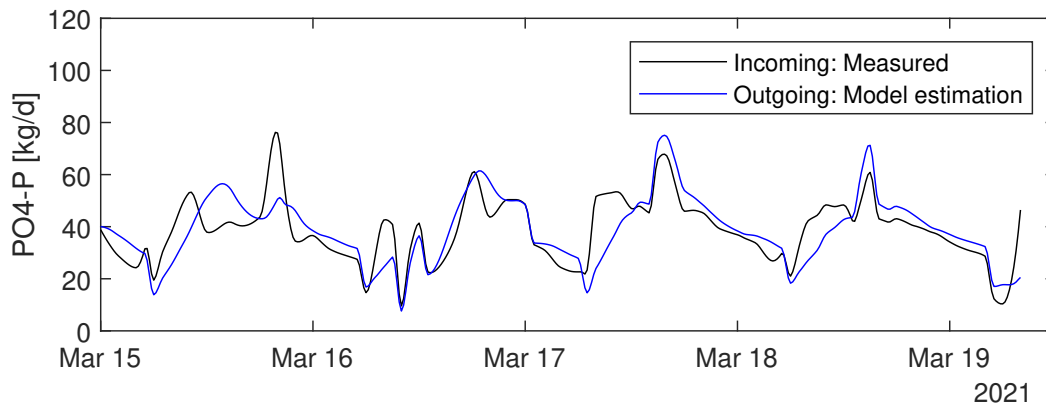


Figure 23: Mass balance over phosphate load.

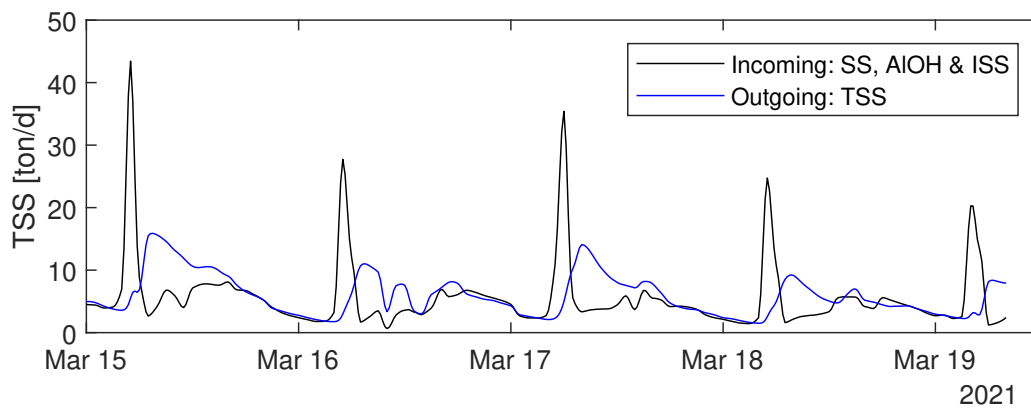


Figure 24: Mass balance over total suspended solids.

The correction factor removal efficiency,  $f_{\text{corr}}$ , proved to have a great impact on the settling.  $f_{\text{corr}}$  reduces the modelled load of total suspended solids in primary sludge. The selected value for  $f_{\text{corr}}$  is significantly lower than the default value (0.3 vs 0.65). As the modelled overestimated the load in the primary sludge, see figure 15, further reducing  $f_{\text{corr}}$  would have resulted in a better mass balance. However, reducing  $f_{\text{corr}}$  further seemed illogical.

There are two main uncertainties for the calibration of the primary clarifier model. The first regards the decanter which is not included in the mass balances. The contribution of decanter was small, and probably does not have a major impact on the mass balance. However, measured total solids in the primary sludge will likely be somewhat higher due to the contribution of material in the decanter. As the primary clarifier model was calibrated against measured total solids, the percentage difference of 17% is likely somewhat bigger than the calculated.

The second uncertainty is that no consideration is taken to differences between the total suspended solids and total solids. The sensor for total solids is also insensitive for higher loads, which makes the evaluation even more difficult.

## 5.2 Prediction of phosphate

A simplified soft sensor proportional to incoming pH was constructed to predict incoming soluble phosphate concentration to the primary clarifier, described by equa-

tion 40. Figure 25 shows the performance of the calibration of the soft sensor. The prediction follows the dynamics nicely, but does not acknowledge the sharp peak on the 15:th, or the magnitude of the peak on the 17:th. Between 00:00 and 08:00 on the 15:th, the prediction is set to one due to incoming  $\text{pH} < 7$ .

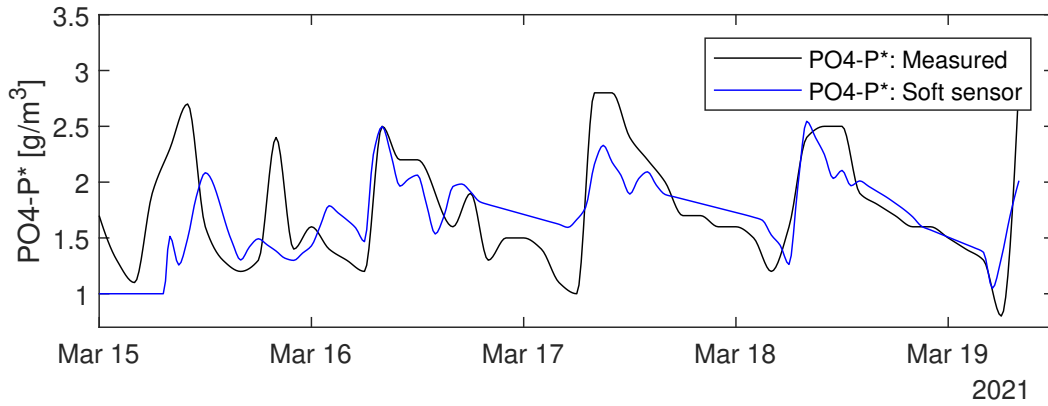


Figure 25: Calibration of the soft sensors prediction of soluble phosphate.

Figure 26 shows the soft sensors performance for the validation data. The prediction captures the dynamic but is overestimated for all points, except at 11:00 on March the 22:nd.

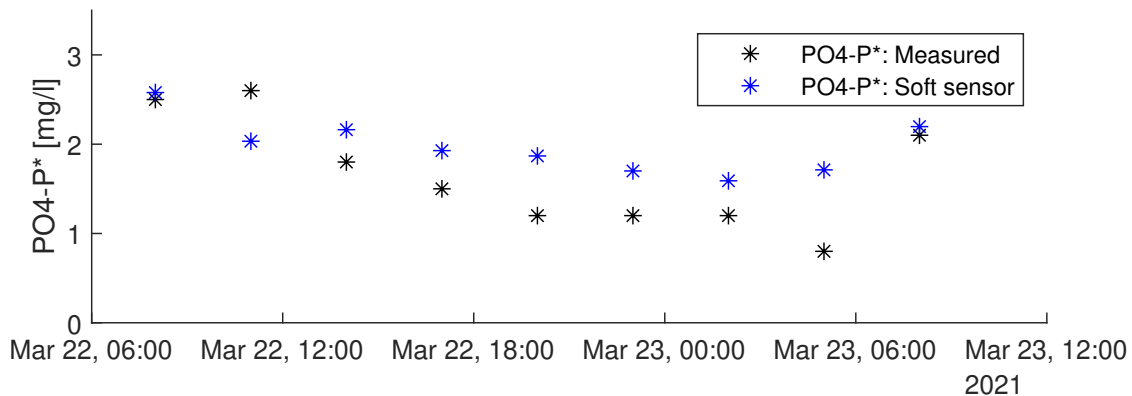


Figure 26: Validation of the soft sensors prediction of soluble phosphate.

Both calibration and validation of the soft sensors performance captures the dynamics of the measured phosphate nicely. However, the prediction tends to underestimate the stretch of the magnitude of the phosphate concentration. This indicates that  $\text{pH}$  alone cannot fully predict incoming phosphate concentration. The prediction also holds one major drawback, which is that the predicted phosphate concentration will be negative when  $\text{pH} < 7$ . For data used in this thesis this could be compensated, but a further development of the correlation is encouraged to avoid this drawback if a soft sensor based on  $\text{pH}$  is to be used in practice.

Even though the simplified soft sensor cannot predict incoming phosphate, the correlation captured the dynamics. One explanation for this correlation is that anaerobic degradation occurs in Regnbågen. Liu et al (2002) investigated a WWTP for snack

food industries. This WWTP faced challenges with a high variation in pH and, likewise Tivoli, used an equalisation tank before the treatment plant. Liu et al (2002) concluded that the large pH derivation derived from hydrolysis in the equalisation tank, caused by long hydraulic retention time. The hydrolysing processes produced volatile fatty acids, VFA, which reduced the pH. There are bacteria known to use VFA for storage of energy. In the process of gathering VFA, the bacteria can release phosphate in the wastewater (SvensktVatten , 2010c). As the settled matter in Regnbågen is only removed during the emptying of Regnbågen, the matter has a long retention time. It is therefore possible that hydrolysing processes are triggered, which could reduce pH within the settled matter. This might be the theoretical explanation of the correlation between pH and incoming phosphate to Tivoli. This theory should be further investigated if pH is to be used as a soft sensor at Tivoli. However, it should also be noted that none of the WWTPs in the national analysis use feedforward control proportional to pH.

It was also surprising that the correlation between suspended solids and phosphate was not better. Several of the WWTPs in the national analyses uses feedforward control proportional to suspended solids with satisfactory results. This might be explained with the settling of material in Regnbågen. During the emptying of Regnbågen, much settled material will enter Tivoli, causing sharp peaks in incoming suspended solids seen in figure 27. Similar peaks can be observed for  $\text{PO}_4\text{-P}^*$  but those are not as obvious.

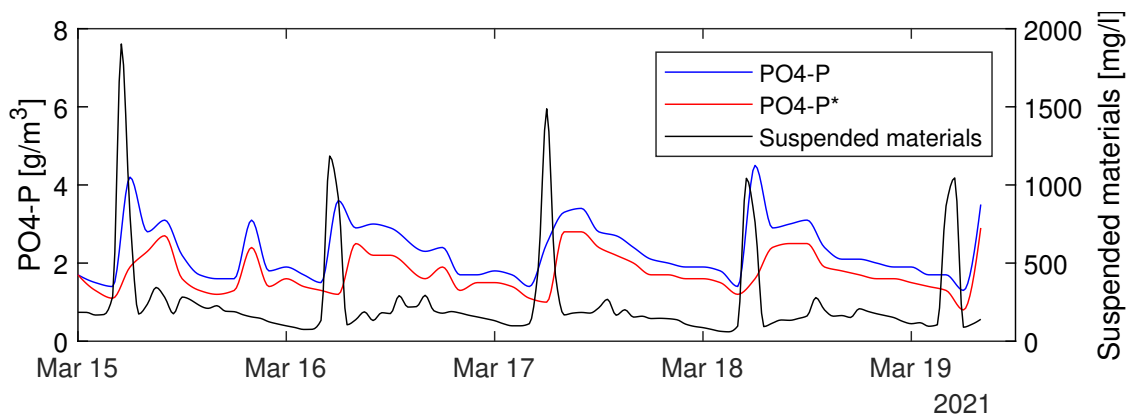


Figure 27: Incoming concentrations of phosphate, soluble phosphate and suspended solids.

This illustrates that Regnbågen reduces the typical correlation between incoming soluble phosphate and suspended solids, as suspended solids settles whereas the dissolved  $\text{PO}_4\text{-P}^*$  does not settle. Due to the settling, incoming suspended solids to Tivoli is more dependent on the clearance of Regnbågen, than of societies activities. As  $\text{PO}_4\text{-P}^*$  does not settle, the concentration depends more of societies activities and therefore follow the flow of wastewater. However, as previously discussed, phosphate is likely released due to anaerobic degradation in Regnbågen, which increases the dissolved phosphate concentration in the lower layers of Regnbågen. Comparing  $\text{PO}_4\text{-P}$  and  $\text{PO}_4\text{-P}^*$  in figure 27 shows that the peaks are more distinct for  $\text{PO}_4\text{-P}$ , than  $\text{PO}_4\text{-P}^*$ . This is probably due to some phosphate is organically bounded, and therefore settles as it is particulate.

### 5.3 Combined feedforward with feedback control

Figure 28 shows that option 3 gives the smallest deviation from the reference value. Increasing the p-value results in bigger oscillation from the reference value (option 2 had highest p-value). The contribution of feedforward could therefore not noticeable allow an higher p-value for feedback control. Increasing  $K_{FFFB}$  reduces the oscillation (option 3 had highest  $K_{FFFB}$ ). This means that it is favourable for the combined control strategy to have a larger contribution of feedforward control.

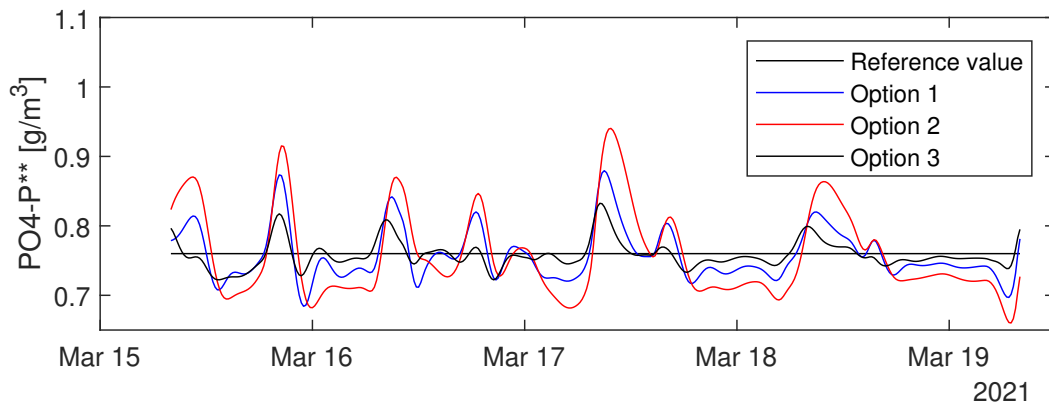


Figure 28: Outgoing phosphate concentration from the primary clarifier for tested values on control parameters.

Option 3 proved to have slightly more rapid changes in coagulant flow compared to option 1 and 2, figure 29. However, as the changes in coagulant flow are quite similar for all options, it could be concluded that option 3 does not have a significant disadvantage regarding changes in coagulant flow. As option 3 resulted in the most stable outgoing phosphate concentration from the primary clarifier, and only scarcely noticeable quicker changes in coagulant flow, it was decided to proceed with option 3.

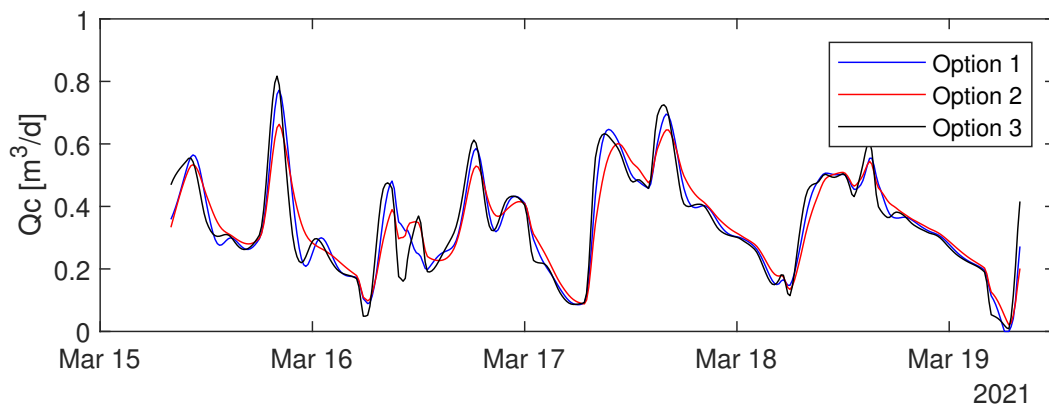


Figure 29: Total coagulant dosage for tested values for control parameters.

Figure 30 shows that feedforward primarily contributes to the total dosage, and that the rapid changes in coagulant flow are mainly due to the feedforward contribution. This is to be expected, as the  $K_{FFFB}$  for option 3 is 0.7.

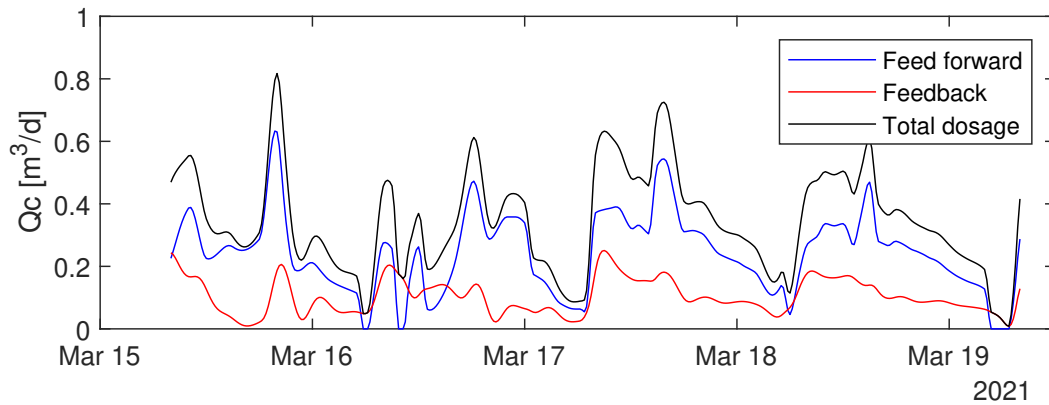


Figure 30: Contribution of feedforward and feedback control to the total coagulant dosage for option 3.

#### 5.4 Evaluation of the control strategies and multi-criteria analysis

Figure 31 shows the modelled outgoing phosphate concentrations for all control strategies, and figure 32 the corresponding chemical dosage. Values for mean value of phosphate, maximum variation of phosphate concentration and coagulant use are shown in appendix 6, table 1.

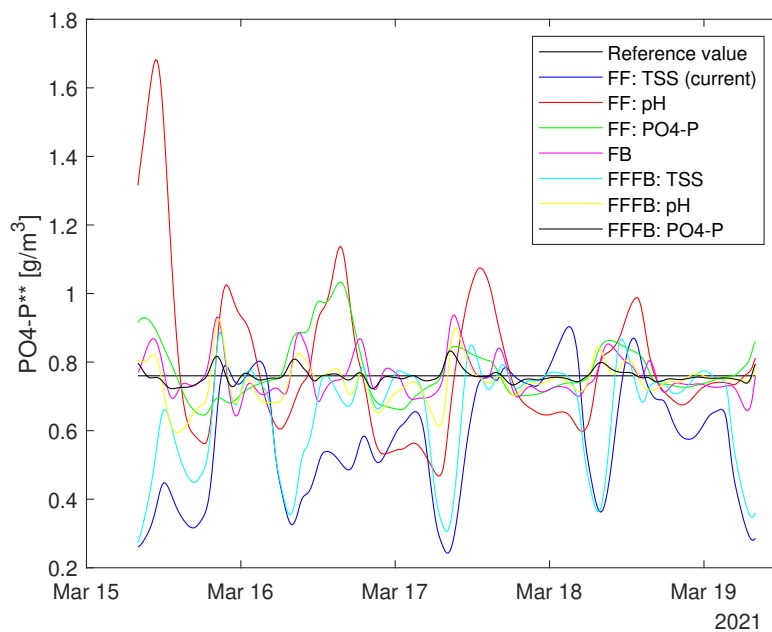


Figure 31: Outgoing phosphate concentrations from the primary clarifier.

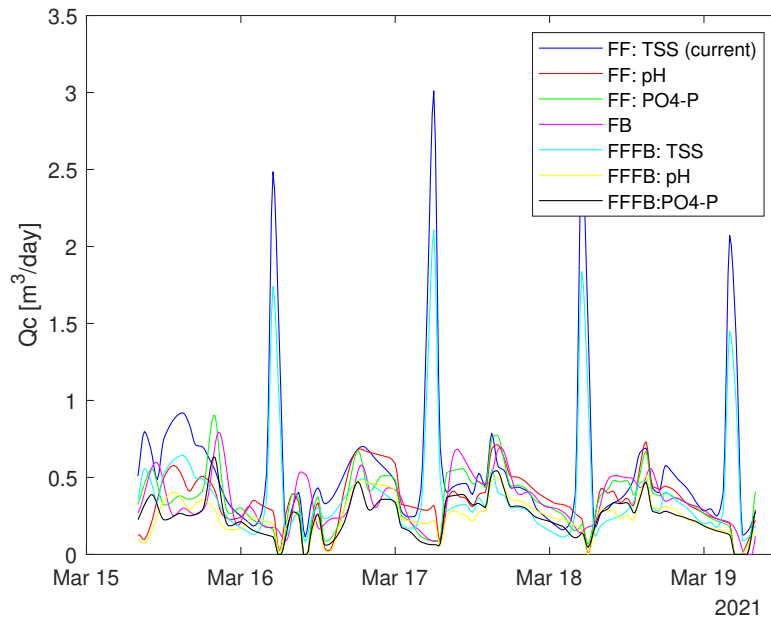


Figure 32: Coagulant flow rate.

It is seen in figure 31 that the control strategies FF & FB: PO<sub>4</sub>-P and FB generate phosphate concentration closest to the reference value. FF alone tend to stray the furthest from the reference value, with the exception of FF: PO<sub>4</sub>-P. FF: pH has the biggest maximum variation of phosphate concentration and FF: TSS is generally much lower than the reference value. All feedforward control strategies are significantly improved when combined with feedback control.

The coagulant flow rate, figure 32, is slightly lower for FF & FB: PO<sub>4</sub>-P, compared to all other control strategies. FF: TSS and FF & FB: TSS have sharp peaks each morning, that are not observed for the other control strategies. The peaks derive from the emptying of Regnbågen, when incoming load increase due to pumping of settled matter to Tivoli WWTP, as seen in figure 27. By comparing figure 31 and 32 it is seen that shortly after the peaks of increased coagulant flow, there is a significant drop in phosphate concentration. This confirms that the current control strategy overdose coagulant during the emptying of Regnbågen, which endangers the bacteria growth during aeration. The current coagulant dosage that FF:TSS represents is, as described, not linear with suspended solids but increases depending on the current water level in Regnbågen.

Table 14 summarises the multi-criteria analysis.

Table 14: Multi-criteria analysis.

Control strategy	Mean value	Max. variation	Coagulant use	Produced sludge	Complexity	Score
FF: TSS	1	3	1	1	4	1.7
FF: pH	2	1	3	4	3	2.4
FF: PO <sub>4</sub> -P	3	4	3	4	3	3.3
FB	4	4	3	4	2	3.45
FF & FB: TSS	1	3	2	3	1	1.85
FF & FB: pH	3	4	3	4	1	3.0
FF & FB: PO <sub>4</sub> -P	4	4	4	4	1	3.55

The highest scoring control strategy from the multi-criteria analysis was FF & FB: PO<sub>4</sub>-P, closely followed by FB. Generally, control strategies including feedback control performed well. Feedforward control for FF: TSS and FF: pH resulted in the lowest and second lowest score, whereas FF: PO<sub>4</sub>-P scored third highest. This indicates that the choice of disturbance that feedforward control is proportional to is of great importance. FB scored higher than all FF control strategies and all FF control strategies were significantly improved when combined with feedback. This implies that implementing feedback control greatly can improve the chemical phosphorus removal at Tivoli.

This conclusion is however largely affected by the choice of interval limits for the multi-criteria analysis, table 13. Interval 4 for the criteria mean value PO<sub>4</sub>-P is achieved if the mean value of PO<sub>4</sub>-P strays no further than  $\pm < 0.01$  [PO<sub>4</sub>-P g/m<sup>3</sup>] from the reference value, which is a very narrow limit. If this limit instead was set to  $\pm < 0.02$  [PO<sub>4</sub>-P g/m<sup>3</sup>] both FF: PO<sub>4</sub>-P and FF & FB: pH would be placed in interval 4, resulting in FF: PO<sub>4</sub>-P would be achieve the highest score with a total point of 3.6. Further increasing the limit to  $\pm < 0.03$  [PO<sub>4</sub>-P g/m<sup>3</sup>] would however have no affect on the outcome of the multi-criteria analysis.

The choice of interval also has a great impact on the maximum variation in phosphate. The maximum variation for FF: pH is significantly wider compared to the other control strategies, which is clear from figure 31 and appendix 6, table 1. Since the intervals are equally divided between the highest and lowest value for each control strategy, the great variation between lowest and highest phosphate concentration from FF: pH increases the range significantly. The intervals are therefore wider, and less sensitive. The same tendency exists also for the criteria coagulant dosage where both FF: TSS and FF & FB: PO<sub>4</sub>-P has deviating values, appendix 6 table 1, and the criteria sludge production. To instead use a linear relationship that could calculate what interval/point the control strategies should achieve based on the control strategies performance, could have made the multi-criteria analysis more sensitive.

The current control strategy, FF: TSS, scored least points and FF & FB: TSS second least in the multi-criteria analysis. This is mainly due to low scores for the criteria mean value of phosphate, which had the highest factor, but also due to low scores for coagulant use and, for FF & FB: TSS, complexity. It should also be noted, that the large

max. variation of phosphate for FF: pH forces both FF: TSS and FF & FB: TSS into interval 3, even though the variation for these two criteria 's is rather large as seen in appendix 6 table 1. This implies that feedforward control proportional to suspended solids is not suitable for Tivoli WWTP. This is probably due to the incoming load of suspended solids during the emptying of Regnbågen does not describe the load of incoming soluble phosphate.

FB performs better than FF: PO<sub>4</sub>-P in terms of matching the reference value. This confirms the conclusion by Ingildsen (2002). However, the coagulant usage was also reduced for Ingildsen (2002) when feedback control was applied, which is not observed in this thesis. Modelled coagulant flow in this thesis for FB is on the contrary slightly higher than FF: PO<sub>4</sub>-P (454 vs 453 [kg/d]), see appendix 6 table 1. In compliance with Liu & Ratnaweera (2016) combining feedforward control with feedback resulted in more stable effluent concentrations and reduced coagulant dosage, compared to only feedforward control.

It is seen in appendix 6 table 1 that the sludge production increases when the coagulant dosage is increased, but the increase of sludge production is only around 1.02% when the coagulant use increases with 1.61 %, calculated from the median value of coagulant use. Reducing coagulant use does not have any affect on the produced sludge. This indicates that the produced sludge is highly dependent on incoming suspended solids present in the wastewater, and that coagulant dosage barely has noticeable affect on the amount of produced sludge.

## 5.5 Consequential errors

### 5.5.1 Estimation of phosphate

Consequential errors from the miss-prediction of phosphate are distinct when evaluating the maximum variation in phosphate concentration. FF: pH has a maximum variation of 1.21, which is nearly double size compared to FF: TSS which has the second biggest maximum variation of 0.66. The large maximum variation for FF: pH deviates from an under-dosage of coagulant causing effluent concentration to increase in the beginning of the simulation, figure 33. This under-dosage derives from a significant miss-prediction of phosphate at the same time, where the predicted incoming phosphate was underestimated, figure 34. By comparing figure 34 and 33, it can be concluded that the greater the difference between measured and predicted phosphate, the further will outgoing phosphate stray from the reference value for FF: pH.

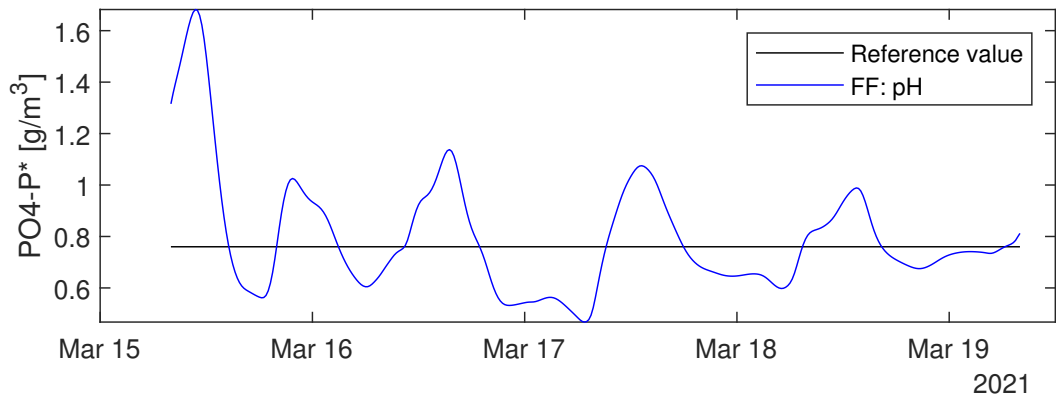


Figure 33: Outgoing phosphate concentration for FF: pH

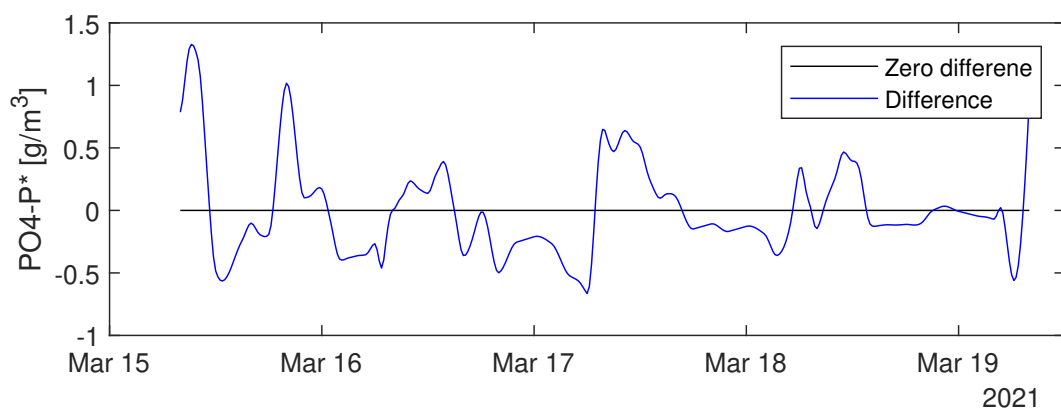


Figure 34: Difference between measured and calculated phosphate from the soft sensor.

### 5.5.2 Comparison over model parameters for ASM2d

Two good alternatives were found when ASM2d was calibrated against  $\text{PO}_4\text{-P}^{**}$ , alternative 2 and alternative 3. As mentioned, alternative 2 has a smaller percentage difference and is therefore used in the thesis. However, as seen in appendix D figure 2, alternative 3 performs better regarding capturing peaks than alternative 2, but alternative 3 tends to overestimate the phosphate concentration. To evaluate whether alternative 3 would have been better, a comparison over alternative 2 and alternative 3 for the highest scoring control strategy, FF & FB:  $\text{PO}_4\text{-P}$ , was conducted. The comparison is seen in figure 35.

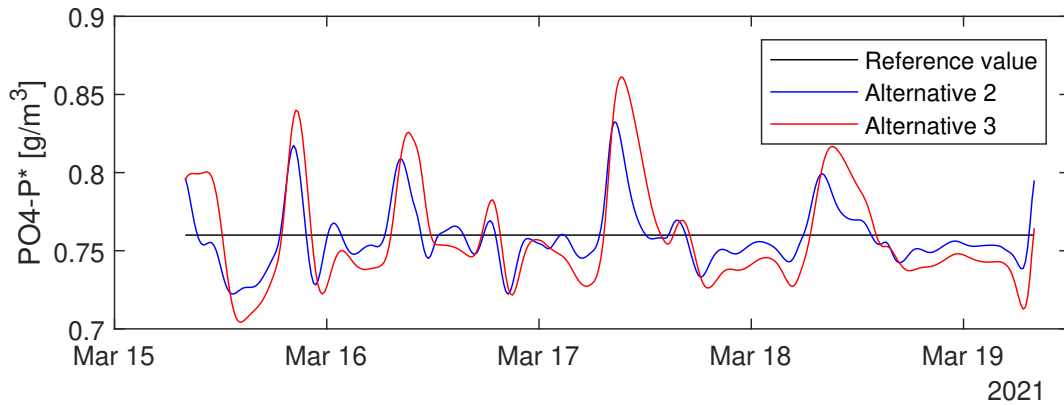


Figure 35: Outgoing phosphate for alternative 2 and 3 from the calibration of ASM2d, for FF & FB:  $\text{PO}_4\text{-P}$ .

Alternative 3 have more dynamics in estimated phosphate concentration compared to alternative 2. Both alternatives had a mean value of  $0.76 \text{ PO}_4\text{-P g/m}^3$ . This indicates that the overestimation of phosphate concentration from alternative 3, seen in appendix D figure 2, is compensated when the optimal control strategy is applied. This implies that alternative 3 would have been better to use, as it preserves the dynamic's and therefore resembles the reality better.

## 5.6 Improvements and uncertainties

Measured data is a probable source of error. Lab samples could stand up to 24 hours in bottles before being analysed. These bottles were not placed within a refrigerator, and it is therefore likely that biological activity occurred which could affect several values of sampled lab data.

Only one of the sand traps was used between the 15:th to the 17:th, which is roughly from start to midway into the sampling campaign. As coagulant is added at the inlet of the sand traps, this might have reduced flocculation due to a higher flow rate of wastewater which could lead to a higher effluent phosphate concentration. However, both measured  $\text{PO}_4\text{-P}$  and  $\text{PO}_4\text{-P}^{**}$  shown in figure 12 are slightly lower during the first half of the sampling campaign. This leads to the conclusion that using only one of the sand traps did not significantly affect measured effluent phosphate concentration, and thereby not modelled phosphate as well.

An uncertainty with the development of  $q_{\text{PAX}, \text{T}}$  is the assumed 1:1 ratio between aluminium and phosphate, based on equation 1. In practice the ratio can be 1-1.5 moles aluminium per mole phosphate. This leads to an underestimation of required coagulant for feedforward control proportional to measured and estimated phosphate load. This does however not explain why steering to suspended solids, FF: TSS and FF & FB: TSS, has a much greater coagulant use, see appendix 6 table 1. The reason why FF: TSS and FF & FB: TSS have greater coagulant use is due to a sharp increase of coagulant flow, figure 32, when incoming load to Tivoli increases during the emptying of Regnbågen. An underestimation of coagulant deriving from the aluminium/phosphate ratio would be continuous throughout the simulation.

The coagulant flow,  $q_{\text{PAX}, \text{R}}$ , is calculated according to equation 45 when feedforward

control is proportional to measured or estimated phosphate load by the soft sensor. The upbringing of equation 45 only regards deviations in incoming phosphate concentration. Investigating deviations in load instead of concentration could possibly improve the calculated coagulant flow. Deviations on load could be investigated likewise as deviations in phosphate concentration was investigated, but changing incoming flow and keep incoming phosphate concentration constant. Equation 45 could be combined with the correlations from deviation in incoming flow.

The best value for the control parameter  $K_{FB}$  was chosen when  $p=0.25$ , which is very low. A greater  $p$ -value resulted in a slow regulator too slow for the system. The reason why the typical  $p$ -values ( $p=1-3$ ) did not work as expected is unclear. One explanation might be that the hydraulic residence time in the primary clarifier has an impact. Problems with long residence time are not uncommon for PI-regulators, and both Ingildsen (2002) & Liu & Ratnaweera (2016) avoided this problematic by placing/modelling their phosphate sensor between the flocculation chamber and the primary clarifier. The reason for this problem is that incoming variation to the primary clarifier can vary quickly, but the residence time is usually quite long, in Tivoli around 2-3 hours. Therefore, measured phosphate concentration at the end of the primary clarifier (from which the process error is calculated from) don't necessarily correspond to the incoming phosphate concentration.

There are therefore several uncertainties and assumptions that make the result less robust. The main issue which impairs the credibility is the choice of interval limit for mean value of phosphate, where small changes alter the outcome of the multi-criteria analyses.

## 6 Conclusions

The purpose of the thesis was to find the optimal control strategy for phosphate precipitation at Tivoli WWTP. Issues resolved are;

1. *Develop a calibrated model that predict the effect of chemical dosage on phosphorus concentration from the primary clarifier.*
2. *Develop a soft sensor that predict incoming soluble phosphate concentration to Tivoli WWTP.*
3. *Determine which control strategy that is most suitable with regard to the stability of the phosphate concentration, coagulant dosage, sludge production and the complexity of the control strategy.*

A calibrated model that can predict the effect of chemical dosage on phosphorus concentration was developed, using ASM2d and a primary clarifier model. ASM2d should be further calibrated to improve the model's estimation of peaks in phosphate concentration. The primary clarifier model was calibrated satisfactory.

A conventional soft sensor was not developed. However, a simplified soft sensor using pH to predict phosphate was developed. This simplified soft sensor cannot satisfactory predict incoming variations of phosphate.

The optimal control strategy is combined feedback and feedforward proportional to incoming measured phosphate, FF & FB:  $PO_4\text{-P}$ .

Additional conclusions are that combining feedforward with feedback control will greatly improve the control strategies performances. Furthermore, the choice of disturbance when feedforward control is implemented, is essential for the control strategies performance. If phosphate concentration cannot be correctly estimated, feedback control alone will have a better performance. The recommended control strategies proposed to Tivoli are presented in order of best expected performance;

1. FF & FB: PO<sub>4</sub>-P. For this control strategy, Tivoli is encouraged to investigate the possibilities to use a sensor that measures incoming soluble phosphate concentration or calibrate a conventional soft sensor.
2. Feedback control. The calculated control parameters should be fine-tuned.
3. FF & FB: pH. For this control strategy, Tivoli is encouraged to further investigate the mathematical and theoretical correlation between pH and incoming phosphate.

## References

- De Haas, D., Wentzel, M.C. & Ekama, G.(2001). The use of simultaneous chemical precipitation in modified activated sludge systems exhibiting biological excess phosphate removal. Part 7: Application of the IAWQ model. *Water S.A* 27(2);151-165.
- Henze, M., Grady, L., Jr., Gujer, W., Marais, G.v.R. & Matsou, T. (1987). Activated sludge model no. 1. *Water Science & technology* A STR No 1, IWA Publishing, London, UK.
- Henze, M., Gujer, W., Takahi, M. & Loosdrecht, M. (2000). Activated sludge models ASM1, ASM2, ASM2d and ASM3. *Water Intelligence Online*. Cornwall: IWA Publishing, London, UK.
- Henze, M., Gujer, W., Mino, T. & Loosdrecht, M. (2002). *Activated sludge models ASM1, ASM2, ASM2d and ASM3*. London: IWA Publishing J.
- Ingeilsen, P. (2002). *Realising Full-Scale Control in Wastewater Treatment Systems Using In Situ Nutrient Sensors*. Diss. Lund University. Department of Industrial Electrical Engineering and Automation. ISBN: 91-88934-22-5.
- IVL. (2008). *Synthesis report on soft sensor activities at Hammarby Sjöstadverket*. (No. B 2306). Stockholm. IVL Swedish Environmental Research Institute.
- Jeppsson, U.(1996). *Modelling Aspects of Wastewater treatment Processes*. . Lund. Institute of technology: Reprocentralen Lund University. ISBN 91-88934-00-4.
- Jeppsson, U., Pons, M.-N., Alex, J., Copp, J.B., Gernaet, K.V., Rosen, C., Steyer, J.-P. Vanrolleghem, P.A.(2007). Benchmark simulation model no 2: general protocol and exploratory case studies. *Water Science & technology*. 56(8);67–78.
- Jeppsson, U., Rosen, C., Alex, J., Copp, J., Germaey, K.V, Pons, M.-N., Vanrolleghem, P.A.(2007). Towards a benchmark simulation model for plant-wide control strategy performant evaluation of WWTPs. *Water Science & technology*. 53(1);287-295.
- Kemira. (2020). *About water treatment*. Helskins.
- Liu, W., Lee, G., Googley, J., Bubel, M., Blank, D. & Moran, S. (2002). Flow Equalization, Hydrolysis and Nutrient Imbalance A Case Study of a Snack Food Industrial Wastewater Treatment Plant. *Water Environment Federation*. 2002(7):291-306.
- Liu, W. & Raanaweera, H. (2016). Improvement of multi-parameter-based feed-forward coagulant dosing control systems with feed-back functionalities. *Water Seine & Technology*. 74(2); 491-499.
- Malovanyy, A. (2015). *Driftinstruktion, Tivoliverket*.
- Manamperuma, L., Liu, W. & Raanaweera, H. (2017). Multi-parameter based coagulant dosing control. *Water Science & Technology*. 75(9); 2157-2162.
- Metcalf & Eddy, Inc. (2014). *Wastewater Engineering- Treatment and Resource Recovery*. 5th ed., New York. McGraw-Hill Professional.
- MittSverige Vatten & Avfall. 2020. *Tivoli Avloppsreningsverk - Miljörapport 2020*.
- Naturvårdsverket. (2017). *Vägledning om maximal genomsnittlig veckobelastning (max gvb)*. Stockholm. Naturvårdsverket. <https://www.naturvardsverket.se/upload/>

stod-i-miljoarbetet/vagledning/avlopp/maximal-genomsnittlig-belastning/vagledningen-om-maximala-genomsnittliga-veckobelastningen.pdf

- Nopens, I., Benedetti, L., Jeppsson, U., Pons, M.-N, Alex, J., Copp, J.B, Germay, K. V., Rosen, C., Steyer, J.-P. Vanrolleghem, P., A. (2010). Benchmark Simulation Model No 2: finalisation of plant layout and default control strategy. *Water science & Technology* 62,(9); 1979-745.
- Otterpohl, R. & Freund, M. (1992). Dynamic models for clarifiers of activated sludge plants with dry and wet weather flows. *Water science & technology* 26(5 -6), 1391-1400.
- Otterpohl, R., Raak, M. and Rolfs, T. (1994). A mathematical model for the efficiency of the primary clarification. *IAWQ 17th Biennial International Conference*, 24- 29 July, Budapest, Hungary.
- Ratnaweera, H. & Fettig, J. (2005). State of the Art of Online monitoring and Control of the Coagulation Process. *Water* 7(11), 6574-6597. <https://doi.org/10.3390/w7116574>.
- SvensktVatten. (2010a). *Avloppsteknik 1- Allmänt*. 2nd ed., Stockholm: Svenskt Vatten AB.
- SvensktVatten. (2010b). *Avloppsteknik 2- Reningsprocessen*. 2nd ed., Stockholm: Svenskt Vatten AB.
- SvensktVatten. (2010c). *Tillämpad reglerteknik och mikrobiologi i kommunala reningsverk*. 2:a uppl., Stockholm: Svenskt Vatten AB.
- SvensktVatten. (2010d). *Avloppsteknik 3- Slamhantering*. 2nd ed., Stockholm: Svenskt Vatten AB.
- Sweco. (2013). *Västerorts framtida avloppshantering*. Delrapport 1: Reningsverk. Stockholm. Stockholm Vatten VA AB.
- Takács, I., Patry, G.G. & Nolasco, D. (1991). A dynamic model of the clarification thickening process. *Water research*, 25(10), 1263- 1271.
- Torkel, G. & Ljung, L. (2006). *Reglerteknik- Grundläggande teori*. 4:e Uppl., Studentlitteratur.
- Vanrolleghem, P., (1999). *Model Based Control of Wastewater Treatment Plants*.
- UNESCO World Water Assessment Program. 2020. *Water and climate change*. United Nations Educational, Scientific, and Cultural Organisation. Paris. ISBN:978-02-3-100371-4 .
- Welch, E. B. (1992). *Ecological effects of wastewater*. 2:a uppl., London: Chapman & Hall.

## Personal communication

Malin Tuveesson. Process and Development Manager at Tivoli WWTP.

Bengt Carlson. Professor at Department of Information Technology, Division of Systems and Control, Uppsala University.

## A Background: National analysis

Table 1: Summarise of the questionnaire for the national analysis.

Treatment plant <i>Organisation and/or city</i>	Load [pe]		Inflow [m <sup>3</sup> /h]		Coagulant
	Current	Max capacity	Current	Max capacity	
- Tivoli <i>MittSverige Vatten&amp; Avfall</i> <i>Sundsvall</i>	50 000	85 000	1000	1100	PAX(AlCl <sub>3</sub> )
- Simsholmen <i>Tekniska kontort, Jönköping</i>	60 000	95 000	1080	1800	FeCl <sub>3</sub>
- Kungsängsverket <i>UppsalaVatten</i>	192 000	200 000	2140	4800	PIX (FeCl <sub>3</sub> )
- Ryaverket <i>Gryvabb, Göteborg</i>	900 000	missing	16 145	14 400	Quickfloc(FeSO <sub>4</sub> )
- Öns avloppsreningsverk <i>Vakin, Umeå</i>	101 700	166 000	1300	2100	PIX(FeCl <sub>3</sub> )
- Käppalaverket <i>Käppalaförbundet, Stockholm</i>	559 000	700 000	6 400	8 700	FeSO <sub>4</sub>
- Himmerfjärdsverket <i>Syöab, Stockholm</i>	224 059	340 000	4000	6000	FeCl <sub>3</sub>
- Göviken <i>Östersunds kommun</i>	65 000	110 000	750	2500	PIX(FeCl <sub>3</sub> )
- Henriksdals reningsverk <i>Stockholm Vatten &amp; Avfall</i>	960 000	missing	12 600	16 200	Quickfloc(FeSO <sub>4</sub> )
- Bromma reningsverk <i>Stockholm Vatten &amp; Avfall</i>	277 000	missing	54000	5700	Winter: PIX(FeCl <sub>3</sub> ) Summer: Quickfloc (FeSO <sub>4</sub> )

## B Method: Data

Data used is seen in figure 1 and 2. Figure 1 shows online data, and figure 2 shows lab measurements.

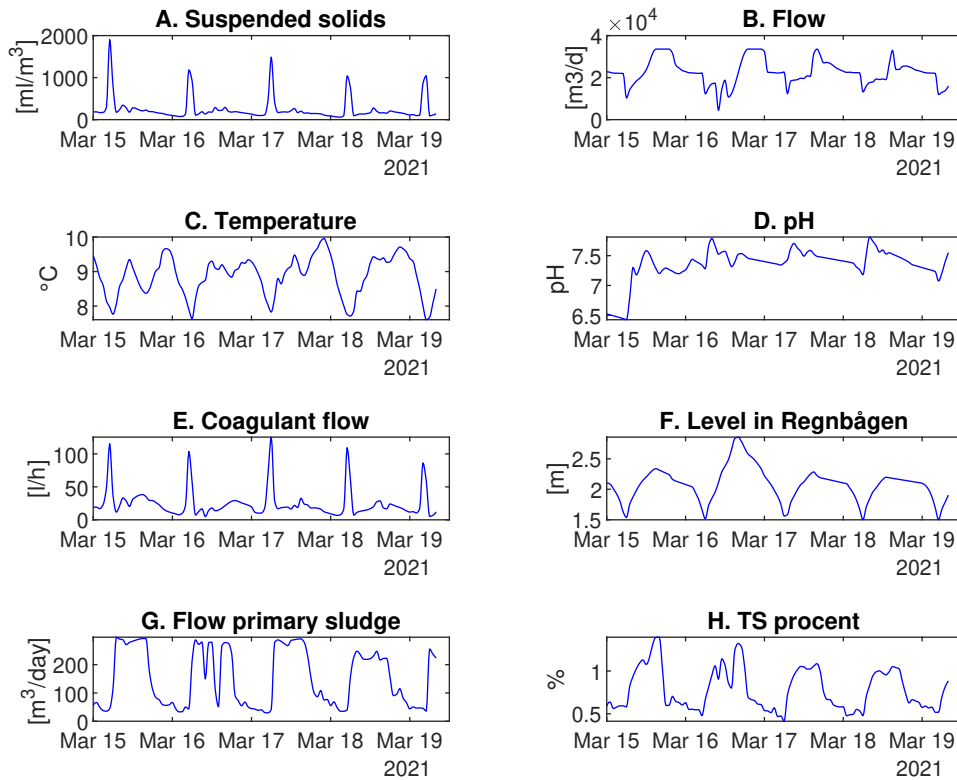


Figure 1: Online data.

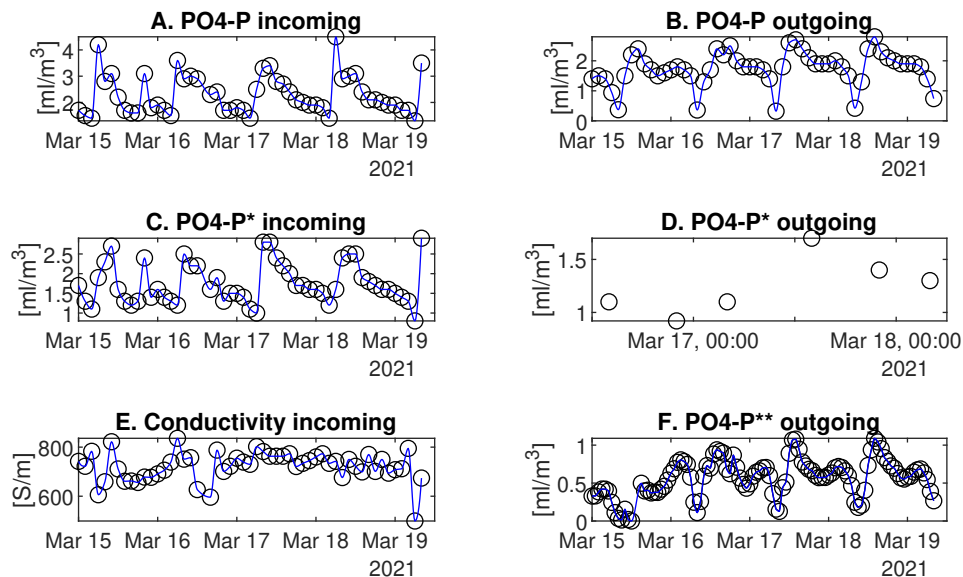


Figure 2: Lab measurements.

## C Method: Soft sensor - prediction of phosphate

Figure 1 shows regression lines when incoming soluble phosphate is plotted against suspended solids, flow, temperature, pH, conductivity and water level in Regnbågen.

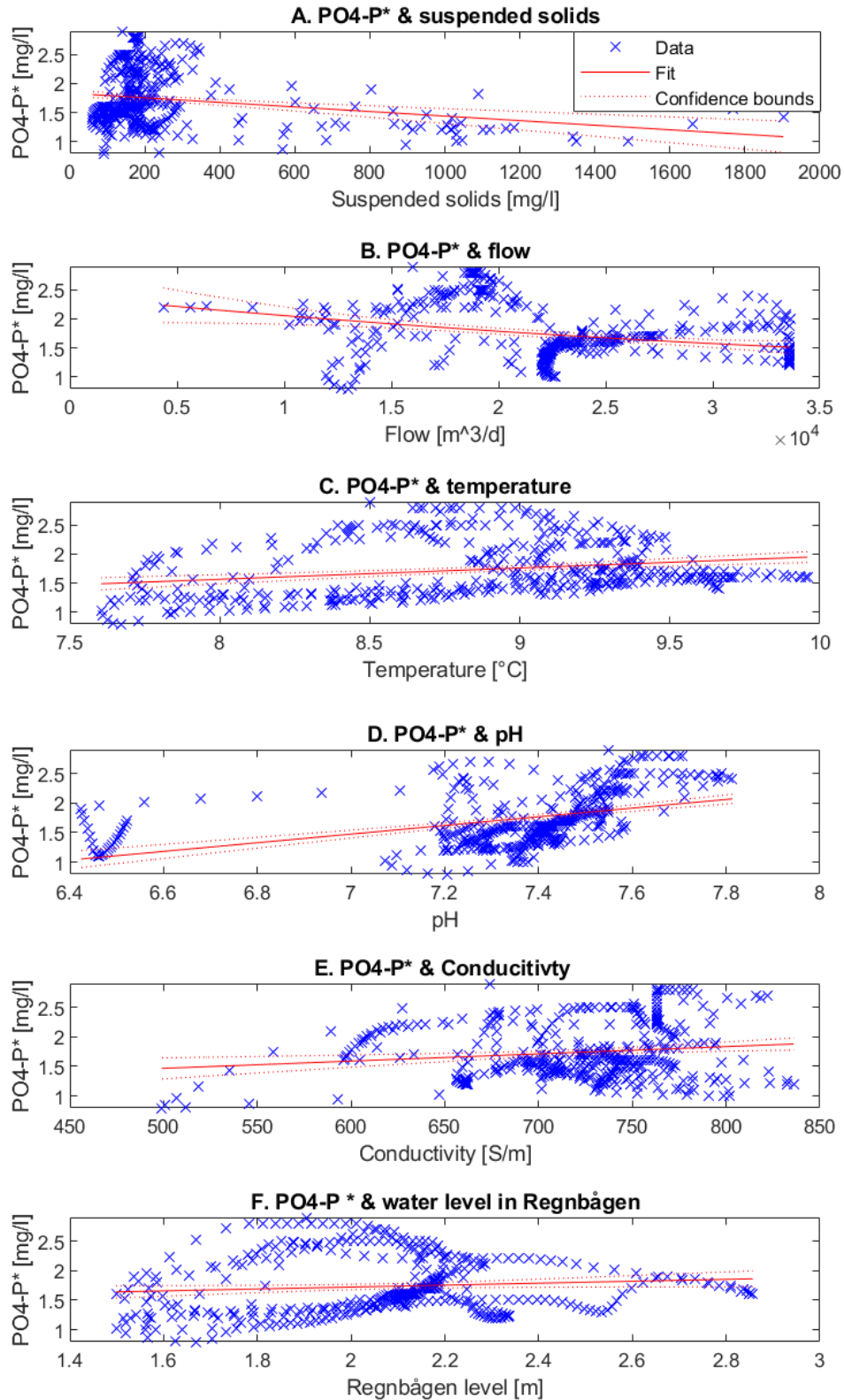


Figure 1. Regression lines.

## D Result: Estimations of phosphate

The historical estimation of effluent soluble  $\text{PO}_4\text{-P}^*$  is seen in figure 1. Figure 2 shows the ASM2d estimation outgoing  $\text{PO}_4\text{-P}^{**}$  for the three calibration alternatives, as well as measured  $\text{PO}_4\text{-P}^{**}$ .

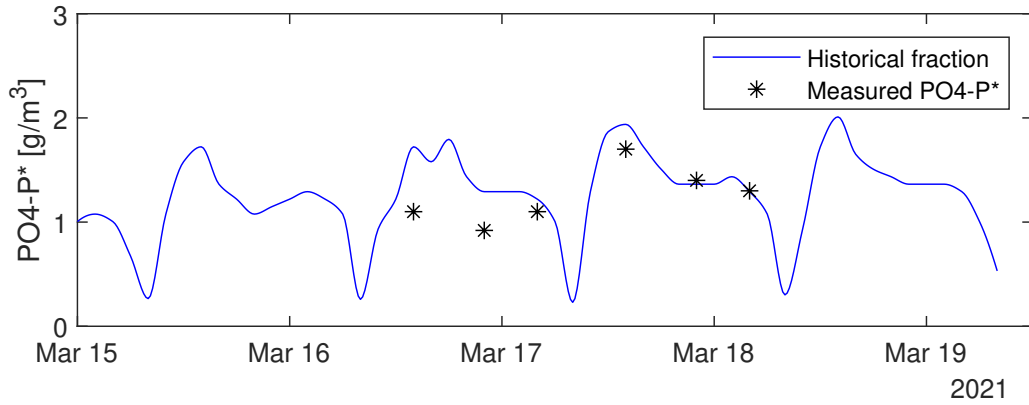


Figure 1. Estimated outgoing  $\text{PO}_4\text{-P}^*$  from primary clarifier.

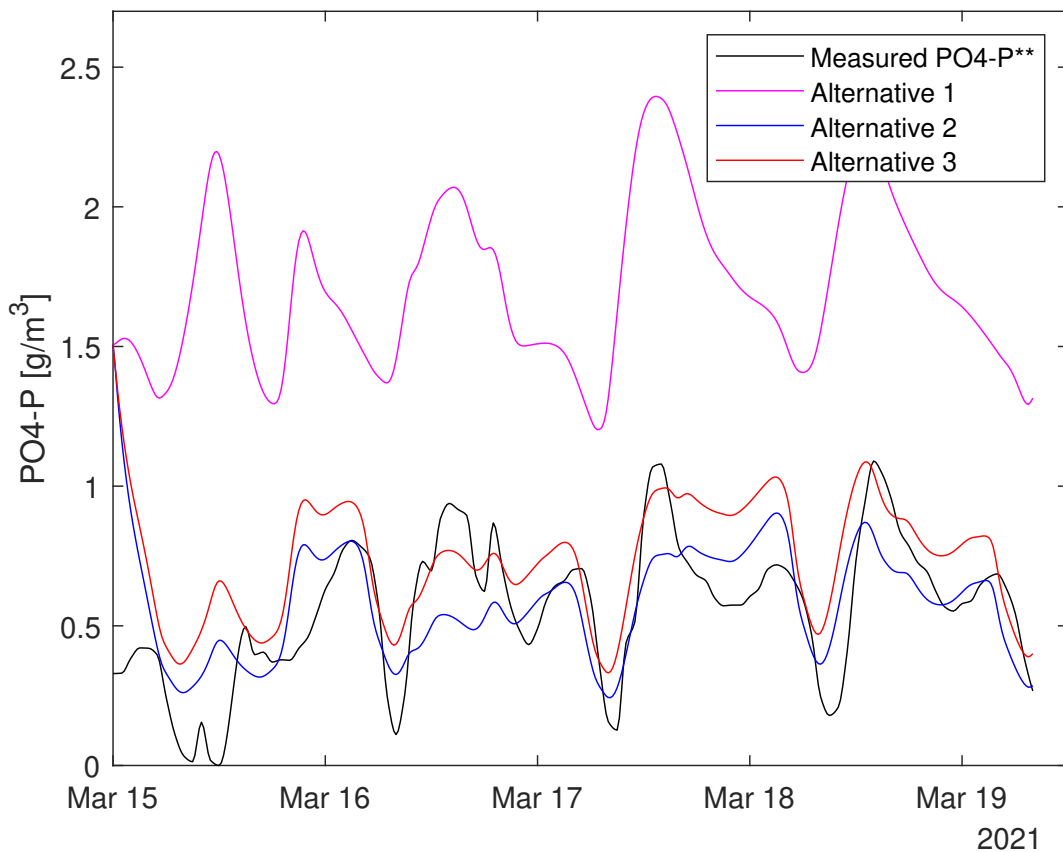


Figure 2. ASM2d estimation of outgoing  $\text{PO}_4\text{-P}^{**}$  from primary clarifier.

## E Result: Performance of the control strategies

Table 1 shows the performance of each criteria for the control strategies.

Table 1: Modelled performance of the control strategies for the multi-criteria analysis.

<b>Control strategy</b>	<b>Mean value</b>	<b>Max. variation</b>	<b>Coagulant use</b>	<b>Produced sludge</b>
	<b>PO<sub>4</sub>-P [g/m<sup>3</sup>]</b>	<b>PO<sub>4</sub>-P [g/m<sup>3</sup>]</b>	<b>[kg/day]</b>	<b>[ton/day]</b>
FF: TSS	0.58	0.66	750	507.9
FF: pH	0.80	1.21	465	499.8
FF: PO <sub>4</sub> -P	0.78	0.39	453	499.8
FB	0.76	0.29	454	500.0
FF & FB: TSS	0.65	0.61	606	503.3
FF & FB: pH	0.74	0.33	471	499.9
FF & FB: PO <sub>4</sub> -P	0.76	0.11	317	499.9